

1 **1. Title page:**

2

3 **Complex controls on nitrous oxide flux across a large elevation gradient in the tropical**
4 **Peruvian Andes**

5

6 Torsten Diem^{1,2}, Nicholas J. Morley¹, Adan Julian Ccahuana³, Lidia Priscila Huaraca Quispe³,
7 Elizabeth M. Baggs⁴, Patrick Meir^{5,6}, Mark I.A. Richards¹, Pete Smith¹, and Yit Arn Teh^{1,2*}

8

9 ¹ School of Biological Sciences, University of Aberdeen, UK

10 ² Formerly at the School of Geography and Geosciences, University of St Andrews, UK

11 ³ Universidad Nacional de San Antonio Abad del Cusco, Peru

12 ⁴ The Royal (Dick) School of Veterinary Studies, University of Edinburgh

13 ⁵ School of GeoSciences, University of Edinburgh, UK

14 ⁶ Research School of Biology, Australian National University, Canberra, Australia

15

16 * Corresponding author; yateh@abdn.ac.uk

17 **2. Abstract**

18 Current bottom-up process models suggest that montane tropical ecosystems are weak
19 atmospheric sources of N₂O, although recent empirical studies from the southern Peruvian
20 Andes have challenged this idea. Here we report N₂O flux from combined field and
21 laboratory experiments that investigated the process-based controls on N₂O flux from
22 montane ecosystems across a large elevation gradient (600-3700 m a.s.l.) in the southern
23 Peruvian Andes. Nitrous oxide flux and environmental variables were quantified in four
24 major habitats (premontane forest, lower montane forest, upper montane forest and
25 montane grassland) at monthly intervals over a 30-month period from January 2011 to June
26 2013. The role of soil moisture content in regulating N₂O flux was investigated through a
27 manipulative, laboratory-based ¹⁵N-tracer experiment. The role of substrate availability
28 (labile organic matter, NO₃⁻) in regulating N₂O flux was examined through a field-based litter-
29 fall manipulation experiment and a laboratory-based ¹⁵N-NO₃⁻ addition study, respectively.
30 Ecosystems in this region were net atmospheric sources of N₂O, with an unweighted mean
31 flux of 0.27 ± 0.07 mg N-N₂O m⁻² d⁻¹. Weighted extrapolations, which accounted for
32 differences in land surface area among habitats and variations in flux between seasons,
33 predicted a mean annual flux of 1.27 ± 0.33 kg N₂O-N ha⁻¹ year⁻¹. Nitrous oxide flux was
34 greatest from premontane forest, with an unweighted mean flux of 0.75 ± 0.18 mg N-N₂O m⁻²
35 d⁻¹, translating to a weighted annual flux of 0.66 ± 0.16 kg N₂O-N ha⁻¹ year⁻¹. In contrast,
36 N₂O flux was significantly lower in other habitats. The unweighted mean fluxes for lower
37 montane forest, montane grasslands, and upper montane forest were 0.46 ± 0.24 mg N-N₂O
38 m⁻² d⁻¹, 0.07 ± 0.08 mg N-N₂O m⁻² d⁻¹, and 0.04 ± 0.07 mg N-N₂O m⁻² d⁻¹, respectively. This
39 corresponds to weighted annual fluxes of 0.52 ± 0.27 kg N₂O-N ha⁻¹ year⁻¹, 0.05 ± 0.06 kg
40 N₂O-N ha⁻¹ year⁻¹, and 0.04 ± 0.07 kg N₂O-N ha⁻¹ year⁻¹, respectively. Nitrous oxide flux
41 showed weak seasonal variation across the region; only lower montane forest showed
42 significantly higher N₂O flux during the dry season compared to wet season. Manipulation of
43 soil moisture content in the laboratory indicated that N₂O flux was significantly influenced by
44 changes in water-filled pore space (WFPS). The relationship between N₂O flux and WFPS was
45 complex and non-linear, diverging from theoretical predictions of how WFPS relates to N₂O
46 flux. Nitrification made a negligible contribution to N₂O flux, irrespective of soil moisture
47 content, indicating that nitrate reduction was the dominant source of N₂O. Analysis of the
48 pooled data indicated that N₂O flux was greatest at 90 and 50 % WFPS, and lowest at 70 and

49 30 % WFPS. This trend in N₂O flux suggests a complex relationship between WFPS and
50 nitrate-reducing processes (i.e. denitrification, dissimilatory nitrate reduction to
51 ammonium). Changes in labile organic matter inputs, through the manipulation of leaf litter-
52 fall, did not alter N₂O flux. Comprehensive analysis of field and laboratory data
53 demonstrated that variations in NO₃⁻ availability strongly constrained N₂O flux. Habitat – a
54 proxy for NO₃⁻ availability under field conditions – was the best predictor for N₂O flux, with
55 N-rich habitats (premontane forest, lower montane forest) showing significantly higher N₂O
56 flux than N-poor habitats (upper montane forest, montane grassland). Yet, N₂O flux did not
57 respond to short-term changes in NO₃⁻ concentration.

58
59

60 **3. Introduction**

61 The tropics are the largest source of atmospheric nitrous oxide (N₂O), accounting for at least
62 half of all global N₂O emissions (Hirsch et al., 2006;Huang et al., 2008;Kort et al.,
63 2011;Nevison et al., 2007;Saikawa et al., 2014). The bulk of tropical N₂O emissions come
64 from terrestrial sources, with the largest emissions arising from agricultural land and
65 unmanaged lowland tropical forests (Hirsch et al., 2006;Huang et al., 2008;Kort et al.,
66 2011;Nevison et al., 2007;Saikawa et al., 2014). However, while we have a relatively robust
67 understanding of the global atmospheric budget as a whole (Hirsch et al., 2006;Huang et al.,
68 2008;Saikawa et al., 2014), our knowledge of regional atmospheric budgets, particularly at
69 the sub-continental scale, is much more limited, due to the constraints imposed by the
70 spatial distribution of existing atmospheric sampling networks and ground-based,
71 ecosystem-scale sampling efforts (Kort et al., 2011;Nevison et al., 2004;Nevison et al.,
72 2007;Saikawa et al., 2014).

73

74 In order to predict and model N₂O flux at these smaller (sub-continental) spatial scales,
75 bottom-up emissions inventories or process-based models are often used, with emissions
76 estimates constrained by empirical measurements (Werner et al., 2007;Li et al., 2000;Potter
77 et al., 1996;Saikawa et al., 2013). However, these models are only as reliable as the data
78 used to parameterize them; as a consequence, ecosystems that are under-represented in
79 the empirical literature or which are poorly understood may be modelled less accurately,
80 with knock-on effects for larger-scale emissions estimates (Saikawa et al., 2013;Teh et al.,

81 2014;Werner et al., 2007). Nitrous oxide dynamics in montane tropical ecosystems are
82 particularly poorly understood, because past research has concentrated on N₂O flux from
83 lowland *tierra firme* forests (Saikawa et al., 2013;Teh et al., 2014;Werner et al., 2007).
84 Montane ecosystems, however, are important components of many tropical landscapes, and
85 account for a sizeable land area. For example, in continental South America, montane
86 ecosystems (>500 m a.s.l.) cover more than 8 % of the land surface (Eva et al., 2004), and
87 play key roles in regional carbon (C), nitrogen (N), and greenhouse gas (GHG) dynamics
88 (Girardin et al., 2010;Moser et al., 2011;Teh et al., 2014;Wolf et al., 2012;Wolf et al., 2011).
89 Process-based models predict that N₂O flux from these montane environments are lower
90 than those from the lowland tropics (i.e. <1.0 kg N₂O-N ha⁻¹ yr⁻¹) (Saikawa et al.,
91 2013;Werner et al., 2007). However, these models have rarely been tested against empirical
92 data, and several field studies indicate that N₂O flux from montane ecosystems can exceed
93 these prior models' estimates (Corre et al., 2010;Teh et al., 2014;Veldkamp et al., 2008). In
94 some instances, N₂O flux from montane ecosystems can in fact approach emissions from
95 lowland forests, begging the question as to whether or not existing models do, in fact,
96 accurately represent flux from these high elevation ecosystems (Corre et al., 2010;Teh et al.,
97 2014;Veldkamp et al., 2008).

98

99 In order to improve our wider understanding of the dynamics and biogeochemistry of N₂O in
100 montane tropical forests, we conducted a combined field and laboratory study to investigate
101 the environmental controls on denitrification and N₂O flux across a large elevation gradient
102 (600-3700 m a.s.l.) in the tropical Peruvian Andes. Prior work from this region indicated that
103 montane ecosystems in this area were stronger sources of N₂O than predicted by bottom-up
104 process models (Teh et al., 2014). In particular, lower elevation premontane and lower
105 montane forests, which account for the majority of the land area in this region (~54 %),
106 showed emission rates that are on par with lowland tropical forests, suggesting that these
107 ecosystems could be important contributors to regional atmospheric budgets (Teh et al.,
108 2014). Nitrous oxide flux appeared to be derived from nitrate reduction (i.e. denitrification,
109 dissimilatory nitrate reduction to ammonium), and was linked to seasonal variations in
110 climate, with N₂O emissions increasing during the dry season compared to the wet season
111 (Teh et al., 2014). However, contrary to theoretical expectations (Davidson, 1991;Firestone
112 and Davidson, 1989;Groffman et al., 2009;Davidson and Verchot, 2000), N₂O flux was not

113 directly correlated with soil moisture content in our field dataset (Teh et al., 2014), raising
114 unresolved questions about the role of seasonal variations in soil moisture content in driving
115 N₂O flux. We hypothesized that the weak relationship between N₂O flux and soil moisture
116 content was because soil water-filled pore space (WFPS) – an index of soil moisture and a
117 proxy for soil anaerobiosis – normally fell above the theoretical threshold where N₂O flux
118 was constrained by the availability of anaerobic microsites (i.e. ~60 % WFPS) in our
119 preliminary dataset (Davidson, 1991; Firestone and Davidson, 1989; Groffman et al.,
120 2009; Davidson and Verchot, 2000; Teh et al., 2014). Even during the dry season, WFPS rarely
121 fell below this threshold value (Teh et al., 2014), allowing other driving variables, such as
122 nitrate (NO₃⁻), to play a more dominant role in regulating N₂O flux (Teh et al., 2014).

123

124 In the work presented here, we extended our time series to multi-annual time scales, in
125 order to better understand the role of longer-term climatic variability in modulating N₂O
126 flux. We also conducted a series of manipulative field and laboratory experiments to
127 investigate the mechanistic controls on N₂O flux in greater detail, and to test hypotheses
128 raised by our earlier work (as described below) (Teh et al., 2014). Furthermore, these
129 manipulative experiments were crucial in helping us interpret our time series of field
130 observations, because prior research indicated that the relationship between individual
131 control variables (e.g. WFPS or NO₃⁻) and N₂O flux were confounded by the simultaneous
132 action of multiple control variables (Teh et al., 2014). The overarching goals of this research
133 were to: investigate how climate and environmental variables regulate N₂O flux over multi-
134 annual time scales; clarify the role of soil moisture as a proximate or distal control on N₂O
135 flux; and evaluate the role of key substrates for nitrate reduction (i.e. labile organic matter,
136 NO₃⁻) in driving N₂O flux. Specifically, we hypothesized that:

137 **H1.** Enhanced N₂O flux during the dry season (i.e. during periods of reduced soil
138 moisture) is due to an increase in N₂O flux from nitrification and reduced N₂O
139 reduction during denitrification

140 **H2.** N₂O flux is poorly correlated with soil water-filled pore space *in situ* because soil
141 moisture content does not normally constrain denitrification under field conditions;
142 however, N₂O flux is closely correlated with water-filled pore space when soil
143 moisture content is more limiting for denitrification (i.e. <60 % WFPS)

144 **H3.** N₂O flux increases proportionately with the availability of substrates for
145 denitrification (i.e. NO₃⁻, labile organic matter)

146 In order to address these three objectives and their attendant hypotheses, we quantified
147 N₂O flux and environmental variables from four major habitat types (premontane forest,
148 lower montane forest, upper montane forest and montane grassland) at monthly intervals
149 over a 30-month period. We also conducted manipulative laboratory experiments that
150 investigated how variations in soil moisture content (WFPS) and NO₃⁻ availability influenced
151 N₂O flux. In addition, we manipulated labile organic matter availability through a field-based
152 litter-fall manipulation study, recognizing that labile organic matter plays an important role
153 in supplying not only the reducing equivalents for nitrate reduction, but also indirectly
154 providing inorganic N for ammonia oxidation and nitrate reduction via N mineralization
155 (Morley and Baggs, 2010; Blackmer and Bremner, 1978; Davidson, 1991; Firestone et al.,
156 1980; Weier et al., 1993).

157

158

159 **4. Materials and methods**

160 **4.1 Study site**

161 Measurements were conducted on the eastern slope of the Andes in the Kosñipata Valley,
162 Manu National Park, Peru (Figure 1) (Malhi et al., 2010). This 3.02 x 10⁶ ha (30,200 km²)
163 region has been the subject of intensive ecological, biogeochemical and climatological
164 studies since 2003 by the Andes Biodiversity and Ecosystem Research Group (or, ABERG;
165 <http://www.andesconservation.org>), and contains a series of long-term permanent plots
166 across a 200-3700 m above sea level (m a.s.l.) elevation gradient that stretches from the
167 western Amazon to the Andes (Malhi et al., 2010). This part of the Andes experiences
168 pronounced seasonality in rainfall but not in air temperature; the dry season extends from
169 May to September and the wet season from October to April (Girardin et al., 2010). Thirteen
170 sampling plots (approximately 20 x 20 m each) were established at four different habitats
171 across a gradient spanning 600-3700 m a.s.l., including premontane forest (600 – 1200 m
172 a.s.l.; n = 3 plots), lower montane forest (1200 – 2200 m a.s.l.; n = 3 plots), upper montane
173 forest (2200 – 3200 m a.s.l.; n = 3 plots), and montane grasslands (3200 – 3700 m a.s.l.; n = 4
174 plots; colloquially referred to as “puna”) (Figure 1). In premontane forest, sampling plots
175 were established in Hacienda Villa Carmen, a 3,065 ha biological reserve operated by the

176 Amazon Conservation Association (ACA), containing a mixture of old-growth forest,
177 secondary forest and agricultural plots (Teh et al., 2014). Sampling for soil gas flux was
178 concentrated in the old-growth portions of the reserve. For lower montane and upper
179 montane forests, sampling plots were established adjacent to or within existing 1 ha
180 permanent sampling plots established by ABERG (Teh et al., 2014). Sampling plots were also
181 established in montane grasslands (Teh et al., 2014). To capture a representative range of
182 environmental conditions, mesotope-scale (100 m-1 km scale landforms) topographic
183 features were sampled (Belyea and Baird, 2006). Mesotopic features include ridges, slopes,
184 flats and a high elevation basin. The latter two landforms include wet, grassy lawns with no
185 discernible grade, and a peat-filled depression, respectively. Summary site descriptions are
186 provided in Table 1. Data on soil properties were collected as part of this study, while mean
187 annual precipitation is from earlier research by ABERG (Girardin et al., 2010).

188

189 **4.2 Soil-atmosphere exchange**

190 Field sampling was performed over a 30-month period from January 2011 to June 2013 for
191 all habitats except for premontane forest. Due to circumstances outside our control, only 24-
192 months of data were collected for premontane forest, with sampling commencing in July
193 2011. Soil-atmosphere flux was collected monthly, except where flooding or landslides
194 prevented safe access by investigators to the study sites. Gas exchange rates were
195 determined with five replicate gas flux chambers deployed in each of the thirteen plots ($n =$
196 65 flux observations per month). All representative landforms were sampled in each habitat
197 (Table 1).

198

199 Soil-atmosphere flux of CH_4 , N_2O and CO_2 were determined using a static flux chamber
200 approach (Livingston and Hutchinson, 1995), although only N_2O flux is reported here.
201 Methane and CO_2 flux are discussed in detail in another publication (Jones et al., 2016).
202 Static flux chamber measurements were made by enclosing a 0.03 m^2 area with cylindrical,
203 opaque (i.e. dark), two-component (i.e. base and lid) vented chambers with a $\sim 8 \text{ L}$ volume.
204 Chamber bases were permanently installed to a depth of approximately 5 cm and inserted
205 >1 month prior to the commencement of sampling, in order to minimize potential artefacts
206 from root mortality following base emplacement (Varner et al., 2003). Chamber lids were
207 fitted with small computer case fans to promote even mixing in the chamber headspace

208 (Pumpanen et al., 2004). Headspace samples were collected from each flux chamber over a
209 30-minute enclosure period, with samples collected at 4 discrete intervals, 7.5 minutes
210 apart, using a gastight syringe. Gas samples were stored in evacuated Exetainers® (Labco
211 Ltd., Lampeter, UK), shipped to the UK by courier, and subsequently analysed for CH₄, N₂O
212 and CO₂ concentrations with a Thermo TRACE GC Ultra (Thermo Fisher Scientific Inc.,
213 Waltham, Massachusetts, USA) at the University of St Andrews. Chromatographic separation
214 was achieved using a Porapak-Q column, and analyte concentrations quantified using a
215 flame ionization detector (FID) for CH₄, electron capture detector (ECD) for N₂O, and
216 methanizer-FID for CO₂. Instrumental precision was determined by repeated analysis of
217 standards and was better than 5 % for all detectors. Gas flux rates were determined using
218 the R HMR package to plot best-fit lines to the data for headspace concentration against
219 time for individual flux chambers (Pedersen et al., 2010; Team, 2012). Gas mixing ratios
220 (ppm) were converted to areal flux by using the Ideal Gas Law to solve for the quantity of gas
221 in the headspace (on a mole or mass basis), normalized by the surface area of each static
222 flux chamber (Livingston and Hutchinson, 1995). Measurements resulting in zero net flux
223 were included in our dataset.

224

225 **4.3 Environmental variables**

226 To investigate the effects of environmental variables on trace gas dynamics, we determined
227 soil moisture, soil oxygen content in the 0-10 cm depth, soil temperature, and air
228 temperature at the time of flux sampling. Volumetric soil moisture content was determined
229 using portable soil moisture probes (ML2x ThetaProbe, Delta-T Device Ltd., Cambridge, UK)
230 inserted into the substrate immediately adjacent to each flux chamber (<5 cm from each
231 chamber base; depth of 0-10 cm). Soil moisture content is reported here as water-filled pore
232 space (WFPS), and is calculated using the measurements of volumetric water content and
233 bulk density (Breuer et al., 2000). Soil O₂ concentration was determined using the approach
234 described by Teh et al. (2014). Soil temperature (0-10 cm depth), chamber temperature and
235 air temperature was determined using type K thermocouples (Omega Engineering Ltd.,
236 Manchester, UK). Data on aboveground litter-fall, meteorological variables (i.e.
237 photosynthetically active radiation, air temperature, relative humidity, rainfall, wind speed,
238 wind direction), continuous plot-level soil moisture (10 and 30 cm depths) and soil

239 temperature (0, 10, 20 and 30 cm depths) measurements were also collected, but are not
240 reported in this publication.

241

242 Resin-extractable inorganic N flux (i.e. ammonium, NH_4^+ ; nitrate, NO_3^-) were quantified in all
243 plots using a resin bag approach (Templer et al., 2005; Subler et al., 1995). From August 2011
244 onwards, ion exchange resin bags (n = 15 resin bags per elevation) were deployed in the
245 plant rooting zone (i.e. 0-10 cm depth in premontane forest, lower montane forest and
246 montane grasslands; 0-15 cm in upper montane forest), following established protocols
247 (Templer et al., 2005; Subler et al., 1995). Samples were collected at monthly intervals
248 (where possible) for determination of monthly, time-averaged NH_4^+ and NO_3^- flux (Subler et
249 al., 1995). For some plots, this sampling frequency was periodically disrupted due to natural
250 hazards (i.e. landslides, river flooding) preventing safe access to the study sites. Resin bags
251 were shipped to the University of Aberdeen after collection from the field, inorganic N was
252 extracted using 2 M KCl and concentrations determined colourimetrically using a Burkard
253 SFA2 continuous-flow analyser (Burkard Scientific Ltd., Uxbridge, UK) (Templer et al.,
254 2005; Subler et al., 1995).

255

256 **4.4 Water-filled pore space manipulation study**

257 We investigated the effects of WFPS on N_2O flux derived from nitrate reduction or
258 nitrification rates using a ^{15}N tracer experiment. Soil cores for all habitats were collected
259 from the 0-10 cm depth, and were not fully air-dried nor sieved prior to incubation. Soils
260 were distributed into glass jars and adjusted to 10% below the target WFPS values of 30%,
261 50%, 70% and 90%, either by letting the soils partially air-dry or by adding water to them,
262 depending on the WFPS of the soils at the time of collection (n = 5 for each ^{15}N addition and
263 3 controls for each WFPS for a total of n = 212; see Table 2). Additional de-ionized water,
264 containing the ^{15}N tracers, was subsequently added gravimetrically to raise WFPS to target
265 levels. The exception to this was for the upper montane forest, where samples were
266 collected from the 0-10 cm depth of the mineral soil, but not from the organic layer. The
267 reason for this is that the mineral soil layer in the upper montane forest is overlain by a thick
268 organic horizon up to 17 cm deep, consisting of poorly decomposed leaves, roots, and humic
269 materials; very akin to low density peat (Zimmermann et al., 2012; Zimmermann et al.,
270 2009a; Zimmermann et al., 2009b). In contrast, the organic matter in the upper 10 cm soil

271 layer in the other habitats is closely intermixed with the mineral phase, and does not
272 normally constitute a distinct mineral-free horizon. Thus, to sample mineral soil in the upper
273 montane forest, we had to sample beneath this thick organic horizon.

274

275 Two different types of ^{15}N -tracers (30 atom %) were applied to the soils in order to
276 determine the proportion of N_2O derived from nitrate reduction and nitrification (Bateman
277 and Baggs, 2005). $^{14}\text{N-NH}_4^{15}\text{N-NO}_3$ was used to quantify the amount of N_2O produced by
278 nitrate reduction, while $^{15}\text{N-NH}_4^{15}\text{N-NO}_3$ was used to quantify the amount of N_2O produced
279 from both nitrate reduction and nitrification. The difference between the two was used to
280 calculate the amount of N_2O derived from nitrification alone. After application of the tracers,
281 the jars were sealed, and gas samples taken at 0, 6, 12, 24, 36 and 48 hours to determine
282 rates of gas flux. Nitrous oxide yield was calculated as the ratio of $^{15}\text{N-N}_2\text{O}$ flux : $^{15}\text{N-N}_2\text{O}$ flux
283 + $^{15}\text{N-N}_2$ flux. Soils were sampled at the end of the experiment for NO_3^- concentration,
284 NH_4^+ concentraion, and total C and N content.

285

286 Soil gas concentrations (N_2O , CO_2 and CH_4) were measured on a GC as described in section
287 4.2, while $^{15}\text{N-N}_2$ and $^{15}\text{N-N}_2\text{O}$ were measured on a SerCon 20:20 isotope ratio mass
288 spectrometer equipped with an ANCA TGII pre-concentration module (SerCon Ltd., UK). The
289 coefficient of variation (CV; an index of instrumental precision) for repeated analysis of gas
290 concentration and isotope standards was <5 %. $^{15}\text{N-N}_2\text{O}$ and $^{15}\text{N-N}_2$ fluxes were calculated
291 from the ^{15}N atom percent excess of the samples compared to the controls using the HMR
292 package (Pedersen et al., 2010).

293

294 **4.5 Litter-fall manipulation experiments**

295 We conducted a field-based litter-fall manipulation experiment to test for the effects of
296 variations in labile organic matter availability on trace gas flux. This study took place over a
297 14-month period (April 2012 to June 2013), and consisted of 4 experimental treatments
298 (control, +50 % litter addition, +100 % litter addition, litter removal) implemented across 3
299 habitats (premontane forest, lower montane forest, upper montane forest), with 6 replicate
300 plots per treatment per habitat (each treatment plot was 0.5 x 0.5 m in size; n = 24
301 observations per habitat; n = 72 observations per sampling increment). Leaf litter addition
302 rates for the +50 % and +100 % litter addition treatments were determined based on prior

303 research from this study site, and fell within the natural range of variability observed across
304 this elevational gradient (Girardin et al., 2010).

305

306 Litter-fall for the litter addition treatments was collected monthly in litter baskets ($n = 3$
307 litter baskets per treatment plot for a total of $n = 18$ per habitat). These data were also used
308 to determine the background rates of leaf litter-fall among habitats. For the control, litter
309 inputs simply reflected natural background litter-fall rates. For the +50 % and +100 % litter
310 addition treatments, background litter inputs were supplemented with additional litter
311 taken from the litter baskets. Briefly, wet litter was weighed in the field using portable scale,
312 gently mixed (homogenized), and then re-distributed to the +50 % and +100 % litter addition
313 plots in amounts proportional to the average amount of wet litter that fell into the litter
314 baskets over the course of the month. As a consequence, the amount of litter added in the
315 two litter addition treatments was not fixed but varied according to the natural background
316 rate of litter-fall. For the litter removal treatment, leaf litter was removed from the forest
317 floor at the start of the experiment, and 3mm nylon mesh was placed over the surface of the
318 treatment plot to prevent further litter ingress to the soil surface. Any debris accumulating
319 on the mesh was removed at monthly intervals.

320

321 Trace gas flux and environmental variables were determined at 7 time points over the
322 course of the 14-month experiment using the methods described in section 4.2. In addition,
323 soil moisture (WFPS from the 0-10 cm depth), soil temperature (0-10 cm depth), air
324 temperature, soil gas concentrations (O_2 , CH_4 , N_2O , CO_2) from the 0-10 cm and 20-30 cm
325 depths, litter C, and litter N were determined concomitantly. Litter C and N content was
326 determined on a Carlo-Erba NA 2500 elemental analyser (CE Instruments Ltd, Wigan, UK) at
327 the University of Aberdeen.

328

329 **4.6 Nitrate addition experiment**

330 To quantify the effect of NO_3^- availability on N_2O flux, we conducted a $^{15}N-NO_3^-$ addition
331 experiment. Background concentrations of NO_3^- were determined prior to the start of
332 experiment using soil subsamples ($n = 5$ per elevation), after which the soils from each
333 habitat were divided into three treatment groups, and supplemented with surplus NO_3^-
334 which raised these background levels by +50 %, +100 %, and +150 % (Table 2). The NO_3^-

335 added to the soil in each of the treatments was enriched with ^{15}N in order to trace the
336 conversion of nitrate to gaseous N products ($^{15}\text{N-N}_2\text{O}$, $^{15}\text{N-N}_2$) (Baggs, 2003; Bateman and
337 Baggs, 2005).

338

339 Soil cores were sampled from 0-10 cm for each habitat (n = 6 soil cores per habitat), with the
340 exception for upper montane forest, where two separate sets of cores were collected, one
341 from the organic layer (O horizon; n = 6) and the other from the mineral layer (A horizon; n =
342 6). Soil samples were then shipped to the University of Aberdeen and sampled within one
343 week of arrival. Transport times from Peru to the UK varied between one and two weeks.
344 Five of these soil cores, one for each replicate, were split into four equal parts (3 treatment
345 samples and one control sample) and distributed into 1 L screw top jars (Kilner, UK). A small
346 soil subsample from each core was used to determine WFPS, background NO_3^- content
347 (extracted in 100ml 1M KCl for a 10g soil sample prior to the start of the experiment), as well
348 as total C and N content. If necessary, the samples were gravimetrically amended with water
349 until the cores reached 80% WFPS. Soil cores were kept under constant conditions for 3 days
350 before the start of the experiment to minimize the effects of changing water content on soil
351 processes.

352

353 At the start of the experiment, dissolved ^{15}N -labelled KNO_3 (30 atom %) was added
354 according to the measured NO_3^- concentrations of each core to reach the required NO_3^-
355 concentration for each treatment (Table 2). Initial NO_3^- concentration (prior to ^{15}N addition)
356 averaged (\pm standard error) $157 \pm 12 \mu\text{g N g soil}^{-1}$ for pre-montane forest, $140 \pm 12 \mu\text{g N g}$
357 soil^{-1} for lower montane forest, $19 \pm 7 \mu\text{g N g soil}^{-1}$ for upper montane forest organic layer
358 soil, $18 \pm 5 \mu\text{g N g soil}^{-1}$ for upper montane forest mineral layer soil, and $6 \pm 2 \mu\text{g N g soil}^{-1}$ for
359 montane grassland soil (Table 2). The jars were then sealed with lids fitted with a two-way
360 stopcock to allow for gas sampling. Gas samples were taken with gas tight syringes, and
361 stored in pre-evacuated containers for determination of $^{15}\text{N-N}_2$, $^{15}\text{N-N}_2\text{O}$, N_2O , CO_2 and CH_4
362 content. Isotope samples (150 ml) were stored in 100 mL serum bottles and gas
363 concentration samples (20 ml) were stored in 12 ml Exetainers[®] (Labco Ltd., Lampeter, UK).
364 After gas sampling, the stopcock was opened to allow the sampled air from the jar to be
365 replaced by lab air, and lab air was sampled to allow for correction of the gas concentrations
366 in the jars due to dilution. Samples were taken at 0, 6, 12, 24, 36, and 48 hours, after which

367 the jars were opened and soil was sampled for determination of NO_3^- , NH_4^+ and total C and
368 N. Gas flux, isotopic and elemental concentrations were determined according to the
369 methods described previously.

370

371 **4.7 Statistics**

372 Statistical analyses were performed using JMP IN Version 8 (SAS Institute, Inc., Cary, North
373 Carolina, USA) or R (Team, 2012). Residuals were checked for heteroscedasticity and
374 homogeneity of variances. Where necessary, the data were transformed using a Box-Cox
375 procedure to meet the assumptions of analysis of variance. Analysis of variance (ANOVA) or
376 Generalized Linear Models were used to evaluate the effect of categorical variables (i.e. site,
377 season, topography) on trace gas flux and environmental variables. Analysis of covariance
378 (ANCOVA) was performed on Box-Cox transformed data to investigate the combined effects
379 of categorical variables and environmental factors (e.g. water-filled pore space, soil oxygen
380 content, air temperature, soil temperature, etc.) on trace gas flux. Non-parametric tests
381 were employed where Box-Cox transformation was unable to normalize the data,
382 homogenize the variances, or where the residuals still showed strong trends even after Box-
383 Cox transformation. Means comparisons were performed using Fisher's Least Significant
384 Difference test (Fisher's LSD). Statistical significance was determined at the $P < 0.05$ level,
385 unless otherwise noted. Values are reported as means and standard errors (± 1 SE).
386 Statistical analyses for the field data were conducted on plot-averaged data to avoid pseudo-
387 replication.

388

389

390 **5. Results**

391 **5.1 Variations in N_2O flux among habitats and between seasons**

392 The overall mean N_2O flux for the entire dataset was 0.27 ± 0.07 mg N- N_2O m⁻² d⁻¹, with a
393 range from -8.40 to 75.0 mg N- N_2O m⁻² d⁻¹. We investigated the effect of habitat, season,
394 topography, and the interaction of habitat by season on N_2O flux by using a three-way
395 ANOVA on plot-averaged data ($F_{10,307} = 3.28$, $P < 0.0005$; Supplementary Online Materials
396 Table S1A). We found that there was a significant effect of habitat ($P < 0.003$) and an effect
397 of season at the borderline of statistical significance ($P < 0.07$). However, we found no effect
398 of topography and no habitat by season interaction effect on N_2O flux. Habitat accounted for

399 the largest proportion of variance in the dataset (4.3 %), while season accounted for only 1.0
400 % of the variance (Supplementary Online Materials Table S1A).

401

402 Among habitats, the overall trend was towards the highest flux from premontane forest
403 ($0.75 \pm 0.18 \text{ mg N-N}_2\text{O m}^{-2} \text{ d}^{-1}$), followed by lower montane forest ($0.46 \pm 0.24 \text{ mg N-N}_2\text{O m}^{-2}$
404 d^{-1}), montane grasslands ($0.07 \pm 0.08 \text{ mg N-N}_2\text{O m}^{-2} \text{ d}^{-1}$), and upper montane forest ($0.04 \pm$
405 $0.07 \text{ mg N-N}_2\text{O m}^{-2} \text{ d}^{-1}$) (Figure 2a). Multiple comparisons tests indicated that only
406 premontane forests showed statistically higher flux than the others (Fisher's LSD, $P < 0.05$);
407 while there were numerical differences in mean flux among the other habitats, large
408 variances meant that they had overlapping ranges of flux (Figure 2a).

409

410 The borderline significant effect of season ($P < 0.07$) reflected an overall trend of higher dry
411 season ($0.51 \pm 0.18 \text{ mg N-N}_2\text{O m}^{-2} \text{ d}^{-1}$) compared to wet season flux ($0.15 \pm 0.07 \text{ mg N-N}_2\text{O}$
412 $\text{m}^{-2} \text{ d}^{-1}$) in the pooled dataset (Table 3). However, part of why the effect of season was weak
413 was because only lower montane forest showed significant variability between seasons
414 (Fisher's LSD, $P < 0.05$), while the other three habitats did not show significant seasonal
415 differences in flux (Fisher's LSD, $P < 0.05$).

416

417 Even though the effect of topography alone was not statistically significant, N₂O flux from
418 flat sites were significantly higher ($0.62 \pm 0.28 \text{ mg N-N}_2\text{O m}^{-2} \text{ d}^{-1}$) than from the basin site ($-$
419 $0.18 \pm 0.16 \text{ mg N-N}_2\text{O m}^{-2} \text{ d}^{-1}$) (Fisher's LSD, $P < 0.05$). However, there was no significant
420 difference between flat sites and either slope or ridge sites ($0.24 \pm 0.09 \text{ mg N-N}_2\text{O m}^{-2} \text{ d}^{-1}$ and
421 $0.20 \pm 0.08 \text{ mg N-N}_2\text{O m}^{-2} \text{ d}^{-1}$, respectively) (Fisher's LSD, $P > 0.05$).

422

423 For each habitat, we also compared individual wet and dry seasons against each other using
424 multiple comparisons tests (e.g. dry season 2012 vs wet season 2012; dry season 2012 vs dry
425 season 2013, etc.) to determine if there was significant inter-annual (i.e. year-on-year)
426 variation in N₂O flux among seasons. Consistent with our three-way ANOVA results, we
427 found that only lower montane forest showed significant variation among multiple dry and
428 wet seasons, whereas the other habitats showed no significant trends. For lower montane
429 forest, we observed significantly higher dry season flux in 2011 compared to wet and dry
430 seasons in all other years ($P < 0.05$; Figure 3b).

431

432 **5.2 Variations in environmental conditions among habitats and between seasons**

433 We investigated the effect of habitat, season, topography, and the interaction of habitat by
434 season on environmental variables using a three-way ANOVA on plot-averaged data. The
435 environmental variables examined here were: water-filled pore space (WFPS) in the 0-10 cm
436 depth, gas-phase soil oxygen content in the 0-10 cm depth, soil temperature, air
437 temperature, and resin-extractable inorganic N flux (NH_4^+ , NO_3^-).

438

439 Water-filled pore space varied significantly as a function of habitat, season, habitat by
440 season, and topography ($F_{10,304} = 637.96$, $P < 0.0001$; Table 3; Figure 2b; Figure 3;
441 Supplementary Online Materials Table S1B). Habitat accounted for the largest proportion of
442 variance in the model (78.1 %), followed by season (0.6 %), habitat by season interaction (0.6
443 %), and topography (0.4 %) (Supplementary Online Materials Table S1B). Each habitat
444 differed significantly from the others (Fisher's LSD, $P < 0.05$), with the highest WFPS observed
445 in montane grassland (88.4 ± 0.3 %), followed by premontane forest (51.6 ± 1.3 %), lower
446 montane forest (39.0 ± 0.9 %), and upper montane forest (35.0 ± 1.5 %) (Figure 2b). WFPS
447 varied significantly between seasons (t-Test, $P < 0.05$), with a mean dry season value of 52.1
448 ± 2.4 % compared to a mean wet season value of 59.5 ± 1.6 % (Table 3). The significant
449 habitat by season interaction is due to the fact that some habitats showed seasonal trends in
450 WFPS whereas others did not. Whereas lower montane and upper montane forests all
451 showed a significant reduction in WFPS during the dry season, premontane forest and
452 montane grasslands showed no seasonal differences in WFPS (Table 3, Figure 3). For
453 topography, the main effect was that the basin landform had significantly higher WFPS than
454 the other landforms. The basin landform showed a mean WFPS of 89.3 ± 0.1 % whereas
455 WFPS in other landforms ranged from 51.7 ± 2.2 to 57.7 ± 2.7 %.

456

457 Soil oxygen in the 0-10 cm depth varied significantly as a function of habitat, habitat by
458 season, and topography ($F_{10,242} = 27.70$, $P < 0.0001$; Table 3; Supplementary Online Materials
459 Table S1C). Habitat accounted for the largest proportion of variance in the model (66.9 % of
460 the total variance), followed by topography (8.4 %), habitat by season (3.5 %)
461 (Supplementary Online Materials Table S1C). For habitat, multiple comparisons tests
462 indicated that only montane grasslands showed significantly lower soil O_2 content than the

463 other habitats ($13.5 \pm 0.6 \%$), while the others showed statistically similar soil O_2 values to
464 each other (18.6 ± 0.2 to $19.5 \pm 0.1 \%$; Fisher's LSD, $P < 0.05$). For topography, multiple
465 comparisons tests indicated that the basin landform showed statistically lower soil O_2
466 content than the other landforms ($7.4 \pm 2.3 \%$), whereas the other topographic features
467 showed statistically similar values, ranging from 16.9 ± 0.6 to $18.2 \pm 0.2 \%$ (Fisher's LSD, $P <$
468 0.05). The significant habitat by season interaction was due to the fact that only montane
469 grassland showed a significant difference in O_2 content between wet and dry season,
470 whereas other habitats showed similar soil O_2 values (Table 3).

471
472 For soil temperature, the effects of habitat, season, habitat by season, and topography were
473 all significant ($F_{10,292} = 790.7$, $P < 0.0001$; Supplementary Online Materials Table S1D).
474 Habitat accounted for the largest proportion of variance in the model (85.5 % of the total
475 variance), followed by season (1.4%), habitat by season interaction (0.5 %), and topography
476 (0.3 %) (Supplementary Online Materials Table S1D). Each habitat differed significantly from
477 the others (Fisher's LSD, $P < 0.05$), with the highest soil temperature observed for
478 premontane forest ($20.5 \pm 0.1 \text{ }^\circ\text{C}$), followed by lower montane forest ($17.8 \pm 0.1 \text{ }^\circ\text{C}$), upper
479 montane forest ($11.5 \pm 0.1 \text{ }^\circ\text{C}$), and montane grasslands ($10.6 \pm 0.2 \text{ }^\circ\text{C}$). Soil temperature
480 varied significantly between season (t-Test, $P < 0.05$), with a mean dry season value of $13.9 \pm$
481 $0.4 \text{ }^\circ\text{C}$ compared to a mean wet season value of $15.1 \pm 0.3 \text{ }^\circ\text{C}$. The significant habitat by
482 season interaction is due to the fact that some habitats showed more pronounced seasonal
483 trends in soil temperature than others, although the overall pattern of cooler dry season
484 compared to wet season soil temperatures holds across all habitats (Table 3). For
485 topography, the flat landforms showed significantly higher soil temperatures than the others
486 ($16.0 \pm 0.5 \text{ }^\circ\text{C}$), the basin landform showed significantly lower values ($10.8 \pm 0.4 \text{ }^\circ\text{C}$), whereas
487 ridge and slope landforms showed similar values to each other ($14.3 \pm 0.4 \text{ }^\circ\text{C}$ and 14.7 ± 0.4
488 $^\circ\text{C}$, respectively) (Fisher's LSD, $P < 0.05$).

489
490 For air temperature, only the effect of habitat was significant ($F_{10,292} = 103.2$, $P < 0.0001$;
491 Table 3; Supplementary Online Materials Table S1E). A multiple comparisons test indicated
492 that each habitat showed significantly different temperatures compared to the others
493 (Fisher's LSD, $P < 0.05$). Premontane forest showed the highest air temperatures (21.0 ± 0.3
494 $^\circ\text{C}$), followed by lower montane forest ($18.7 \pm 0.2 \text{ }^\circ\text{C}$), upper montane forest ($12.7 \pm 0.2 \text{ }^\circ\text{C}$),

495 and montane grassland (11.7 ± 0.3 °C). Other variables did not significantly affect air
496 temperature.

497

498 For resin-extractable NH_4^+ flux, even though the three-way ANOVA model was not
499 statistically significant, the overall trend was towards significantly lower NH_4^+ flux in the dry
500 season (9.6 ± 0.7 $\mu\text{g N-NH}_4$ $\text{g resin}^{-1} \text{d}^{-1}$) compared to the wet season (22.3 ± 3.6 $\mu\text{g N-NH}_4$ g
501 $\text{resin}^{-1} \text{d}^{-1}$) ($F_{10,164} = 1.3$, $P > 0.2$; Table 3; Supplementary Online Materials Table S1F).

502

503 Resin-extractable NO_3^- flux showed different patterns from NH_4^+ flux, with significant effects
504 of habitat, topography, and habitat by season but not of season alone ($F_{10,164} = 39.0$, $P <$
505 0.0001 ; Figure 2c; Table 3; Supplementary Online Materials Table S1G). Habitat accounted
506 for the largest proportion of the variance (61.5 %), followed by topography (4.7 %), and
507 habitat by season (1.9 %). Premontane forest showed the highest NO_3^- flux (22.6 ± 2.0 $\mu\text{g N-}$
508 NO_3 $\text{g resin}^{-1} \text{d}^{-1}$), followed by lower montane forest (10.0 ± 1.2 $\mu\text{g N-NO}_3$ $\text{g resin}^{-1} \text{d}^{-1}$)
509 (Fisher's LSD, $P < 0.05$; Figure 2c). Upper montane forest (1.1 ± 0.2 $\mu\text{g N-NO}_3$ $\text{g resin}^{-1} \text{d}^{-1}$) and
510 montane grassland (1.7 ± 0.3 $\mu\text{g N-NO}_3$ $\text{g resin}^{-1} \text{d}^{-1}$) showed significantly lower NO_3^- flux than
511 the other two habitats (Fisher's LSD, $P < 0.05$; Figure 2c), with values that were not
512 significantly different from each other (Fisher's LSD, $P > 0.05$; Figure 2c). For the effect of
513 topography, multiple comparisons tests indicated that flat landforms (12.1 ± 1.8 $\mu\text{g N-NO}_3$ g
514 $\text{resin}^{-1} \text{d}^{-1}$) and slope landforms (10.2 ± 1.6 $\mu\text{g N-NO}_3$ $\text{g resin}^{-1} \text{d}^{-1}$) differed significantly from
515 ridge landforms (6.6 ± 1.4 $\mu\text{g N-NO}_3$ $\text{g resin}^{-1} \text{d}^{-1}$) (Fisher's LSD, $P < 0.05$). The basin landform
516 (3.8 ± 1.3 $\mu\text{g N-NO}_3$ $\text{g resin}^{-1} \text{d}^{-1}$), despite the lower mean values, showed an overlapping
517 range with the other landforms (Fisher's LSD, $P > 0.05$). The habitat by season interaction
518 was due to the fact that upper montane forest shows a significant seasonal fluctuation in
519 resin-extractable NO_3^- (Fisher's LSD, $P < 0.05$), whereas the other habitats show no significant
520 seasonal trend (Fisher's LSD, $P > 0.05$; Table 3).

521

522 **5.3 Effects of environmental variables on N_2O flux**

523 For the whole dataset, the relationship between N_2O flux and environmental variables was
524 examined using an ANCOVA on Box-Cox transformed data with habitat, season, topography,
525 and environmental variables as covariates. Environmental variables included WFPS, oxygen,
526 air temperature, soil temperature, and resin-extractable inorganic N flux (NH_4^+ and NO_3^-).

527 The ANCOVA model as a whole was not statistically significant ($P > 0.4$). However, we found
528 that individual factors were weakly but significantly correlated with N_2O flux for the pooled
529 dataset. These included soil temperature ($r^2 = 0.04$, $P < 0.0004$), air temperature ($r^2 = 0.04$, P
530 < 0.0008), and resin-extractable NO_3^- flux ($r^2 = 0.03$, $P < 0.03$). Water-filled pore space also
531 showed a very weak negative correlation with N_2O flux at the borderline of statistical
532 significance ($r^2 = 0.01$, $P < 0.06$).

533

534 For individual habitats, we explored how variations in environmental conditions influenced
535 N_2O flux using multiple regression, with WFPS, oxygen, soil temperature, air temperature,
536 resin-extractable NH_4^+ flux, and resin-extractable NO_3^- flux as explanatory variables. Only the
537 multiple regression analysis for lower montane forest showed a borderline significant result,
538 though only at the $P < 0.07$ level ($r^2 = 0.36$). The multiple regression models for all the other
539 habitats were not statistically significant ($P > 0.4$). Lower montane forest was the only
540 habitat that showed a significant effect of season on N_2O flux (section 5.1), and our multiple
541 regression model corroborated this result by showing that seasonal fluctuations in air
542 temperature, soil temperature, WFPS (Figure 3b), and NH_4^+ all correlated with N_2O flux ($P <$
543 0.05). Air temperature explained the largest proportion of variance in the data (26.2 %;
544 negative trend), followed by soil temperature (15.5 %; positive trend), WFPS (13.7 %;
545 negative trend), and resin-extractable NH_4^+ flux (11.6 %; negative trend).

546

547 **5.4 Water-filled pore space manipulation**

548 $^{15}N-N_2O$ and $^{15}N-N_2$ fluxes showed a biphasic response (Limmer and Steele, 1982), with
549 significantly different flux rates in the first 24 hours of incubation compared to the later
550 period of incubation (i.e. 24-48 hours). Flux of $^{15}N-N_2O$, and $^{15}N-N_2$ were therefore divided
551 into early (0-24 hours) and late (24-48 hours) phase flux.

552

553 **5.4.1 Role of nitrification and nitrate reduction in N_2O production**

554 The ^{15}N flux data indicates that nitrate reduction (i.e. denitrification) was the dominant
555 source of N_2O from these soils, while nitrification was only a minor contributor to $^{15}N-N_2O$
556 production (Supplementary Online Materials Figure S1). The $^{15}N-N_2O$ and $^{15}N-N_2$ fluxes were
557 analyzed using a full factorial ANOVA on Box-Cox transformed data with habitat, moisture
558 level, form of ^{15}N -label added (i.e. $^{15}NH_4^{15}NO_3$ or $^{14}NH_4^{15}NO_3$), incubation phase, and all their

559 interaction terms as independent variables. Notably, this analysis revealed that the form of
560 ^{15}N -label added (i.e. $^{15}\text{N-NH}_4$ $^{15}\text{N-NO}_3$ or $^{14}\text{N-NH}_4$ $^{15}\text{N-NO}_3$) did not significantly alter $^{15}\text{N-N}_2\text{O}$
561 flux, indicating that production of $^{15}\text{N-N}_2\text{O}$ from nitrification was weak to negligible
562 (Supplementary Online Materials Figure S1). In order to simplify our statistical analyses, all
563 subsequent analyses were performed using only habitat, moisture level, incubation phase,
564 and their interaction terms as independent variables. For these tests, which are described
565 below, the “total” flux of $^{15}\text{N-N}_2\text{O}$ or $^{15}\text{N-N}_2$ represents gas produced by both nitrification
566 and nitrate reduction.

567

568 **5.4.2 $^{15}\text{N-N}_2\text{O}$ flux**

569 For the total $^{15}\text{N-N}_2\text{O}$ flux data, we used a full factorial ANOVA on Box-Cox transformed data
570 with habitat, moisture level, incubation phase, and all their interactions as independent
571 variables. We found that moisture level, habitat by incubation phase, and habitat by
572 moisture by incubation phase were significantly related to $^{15}\text{N-N}_2\text{O}$ flux (ANOVA, $F_{31, 321} =$
573 3.06 , $P < 0.0001$; Figure 4; Supplementary Online Materials Table S2A). Of the three main
574 factors (i.e. habitat, moisture level, incubation phase), moisture level was the dominant
575 control on $^{15}\text{N-N}_2\text{O}$ flux (Supplementary Online Materials Table S2A). The highest $^{15}\text{N-N}_2\text{O}$
576 flux was observed in the 90 % WFPS ($42 \pm 9 \text{ ng N}_2\text{O-}^{15}\text{N g}^{-1} \text{ d}^{-1}$) and 50 % WFPS ($29 \pm 10 \text{ ng}$
577 $\text{N}_2\text{O-}^{15}\text{N g}^{-1} \text{ d}^{-1}$) treatments, and the lowest flux in the 30 % ($3 \pm 1 \text{ ng N}_2\text{O-}^{15}\text{N g}^{-1} \text{ d}^{-1}$) and 70
578 % ($7 \pm 2 \text{ ng N}_2\text{O-}^{15}\text{N g}^{-1} \text{ d}^{-1}$) treatments (Fisher’s LSD, $P < 0.05$; Figure 4). The habitat by
579 incubation phase interaction indicated that some habitats showed different flux rates during
580 early and late phases of the incubation (Figure 4). Premontane and lower montane forest
581 showed statistically similar $^{15}\text{N-N}_2\text{O}$ flux during early and late incubation phases. Upper
582 montane forest mineral layer soils showed a significant increase in $^{15}\text{N-N}_2\text{O}$ flux from early to
583 late incubation phases ($5 \pm 2 \text{ ng N}_2\text{O-}^{15}\text{N g}^{-1} \text{ d}^{-1}$ versus $42 \pm 13 \text{ ng N}_2\text{O-}^{15}\text{N g}^{-1} \text{ d}^{-1}$; t-Test, $P <$
584 0.003), while montane grasslands showed a significant decrease in $^{15}\text{N-N}_2\text{O}$ flux from early to
585 late incubation phases ($60 \pm 23 \text{ ng N}_2\text{O-}^{15}\text{N g}^{-1} \text{ d}^{-1}$ versus $6 \pm 9 \text{ ng N}_2\text{O-}^{15}\text{N g}^{-1} \text{ d}^{-1}$, respectively;
586 t-Test, $P < 0.02$). The habitat by moisture by incubation phase effect stems from complex
587 and varying responses of soils from different habitats to differences in moisture level and
588 incubation phase (Figure 4).

589

590 **5.4.3 $^{15}\text{N-N}_2$ flux**

591 For the total $^{15}\text{N-N}_2$ flux data, we used a full factorial ANOVA on Box-Cox transformed data
592 with habitat, moisture level, incubation phase, and all their interactions as independent
593 variables. We found that all of the main factors and their interaction terms were statistically
594 significant (ANOVA, $F_{31,317} = 14.20$, $P < 0.0001$; Supplementary Online Materials Table S2B).
595 Of the three main factors, habitat was the dominant control on $^{15}\text{N-N}_2$ flux (Supplementary
596 Online Materials Table S2B). Lower montane forest showed the highest $^{15}\text{N-N}_2$ flux (694 ± 83
597 $\text{ng N}_2\text{-}^{15}\text{N g}^{-1} \text{d}^{-1}$); premontane forest and upper montane forest mineral layer soil showed
598 intermediate levels of flux (326 ± 53 and $171 \pm 20 \text{ ng N}_2\text{-}^{15}\text{N g}^{-1} \text{d}^{-1}$, respectively); and
599 montane grassland soil showed the lowest flux ($123 \pm 23 \text{ ng N}_2\text{-}^{15}\text{N g}^{-1} \text{d}^{-1}$) (Fisher's LSD, $P <$
600 0.05 ; Figure 4). Moisture played a secondary role in regulating $^{15}\text{N-N}_2$ flux (Supplementary
601 Online Materials Table S2B), with only the 90 % treatment had significantly higher flux than
602 the other treatments (90 % WFPS treatment: $437 \pm 77 \text{ ng N}_2\text{-}^{15}\text{N g}^{-1} \text{d}^{-1}$; pooled average for
603 all other treatments: $294 \pm 28 \text{ ng N}_2\text{-}^{15}\text{N g}^{-1} \text{d}^{-1}$) (Fisher's LSD, $P < 0.05$). Incubation phase was
604 the least important control on $^{15}\text{N-N}_2$ flux, with slightly greater flux of $^{15}\text{N-N}_2$ during the late
605 compared to the early phase of the incubations ($373 \pm 44 \text{ ng N}_2\text{-}^{15}\text{N g}^{-1} \text{d}^{-1}$ versus $288 \pm 37 \text{ ng}$
606 $\text{N}_2\text{-}^{15}\text{N g}^{-1} \text{d}^{-1}$) (t-Test, $P < 0.07$). The habitat by moisture level interaction indicates that flux
607 from different habitats showed varying moisture responses (Figure 4). For example, $^{15}\text{N-N}_2$
608 flux from premontane forest and upper montane forest mineral layer soil showed no
609 responses to moisture. In contrast, for lower montane forest, flux was greatest for the 90 %
610 WFPS treatment ($1,365 \pm 201 \text{ ng N}_2\text{-}^{15}\text{N g}^{-1} \text{d}^{-1}$), lowest for the 70 % WFPS treatment ($257 \pm$
611 $128 \text{ ng N}_2\text{-}^{15}\text{N g}^{-1} \text{d}^{-1}$), and at intermediate levels for the 30 and 50 % WFPS treatments ($664 \pm$
612 131 and $492 \pm 79 \text{ ng N}_2\text{-}^{15}\text{N g}^{-1} \text{d}^{-1}$, respectively) (Fisher's LSD, $P < 0.05$). The pattern for
613 montane grassland was different again; here, only the 90 % WFPS treatment showed
614 significantly greater flux ($171 \pm 32 \text{ ng N}_2\text{-}^{15}\text{N g}^{-1} \text{d}^{-1}$) compared to the other treatments
615 (pooled average: $105 \pm 29 \text{ ng N}_2\text{-}^{15}\text{N g}^{-1} \text{d}^{-1}$) (Fisher's LSD, $P < 0.05$).

616

617 **5.4.4 N₂O Yield**

618 For the N₂O yield, we used a full factorial ANOVA on Box-Cox transformed data with habitat,
619 moisture level, incubation phase, and all their interactions as independent variables. We
620 found that habitat, moisture level, habitat by moisture level, habitat by phase, and habitat
621 by moisture level by phase significantly influenced N₂O yield (ANOVA, $F_{31,313} = 9.85$, $P <$
622 0.0001 ; Supplementary Online Materials Table S2C). Of the three main factors, habitat was

623 the best predictor of N₂O yield (Supplementary Online Materials Table S2C). N₂O yield was
624 highest for the montane grassland (0.61 ± 0.06), lowest for lower montane forest ($0.19 \pm$
625 0.04), while premontane forest and upper montane forest mineral layer soil showed similar
626 intermediate values (0.40 ± 0.05 and 0.42 ± 0.05 , respectively) (Fisher's LSD, $P < 0.05$).
627 Moisture level explained much less of the variance in the dataset (Supplementary Online
628 Materials Table S2C); N₂O yield was highest for the 70 % WFPS treatment (0.51 ± 0.06), while
629 the 30, 50 and 90 % WFPS treatments showed statistically similar values (0.35 ± 0.05 , $0.39 \pm$
630 0.05 , and 0.36 ± 0.05 , respectively) (Fisher's LSD, $P < 0.05$). For the habitat by moisture level
631 interaction, this reflects the fact that only lower montane forest and upper montane forest
632 showed differences in N₂O yield with changes in moisture level. For the lower montane
633 forest, N₂O yield was greatest in the 70 % WFPS treatment (0.51 ± 0.11), whereas the other
634 treatments were not statistically different from each other (pooled average: 0.09 ± 0.03)
635 (Fisher's LSD, $P < 0.05$). Upper montane forest mineral layer soil showed the highest N₂O
636 yield for the 90 % treatment (0.72 ± 0.08), lowest yield for the 30 % WFPS treatment ($0.20 \pm$
637 0.09), and intermediate N₂O yields for the 50 and 70 % WFPS treatments (0.29 ± 0.09 and
638 0.50 ± 0.11 , respectively) (Fisher's LSD, $P < 0.05$). For the habitat by incubation phase
639 interaction, this reflects the fact that upper montane forest mineral layer soil showed an
640 increase in N₂O yield from early to late phase, while montane grassland showed a decrease
641 in N₂O yield from early to late phase. The habitat by moisture level by incubation phase
642 interaction reflects the complex and varied responses of soils from different habitats to
643 changes in moisture level and incubation phase (Figure 4).

644

645 **5.5 Litter manipulation experiment**

646 In order to investigate the relationship between leaf litter input rates and N₂O flux, we used
647 a Generalized Linear Model (GLM) and an ANCOVA that included habitat, litter treatment,
648 season, WFPS, litter input rate, litter C input rate, litter N input rate, soil temperature and air
649 temperature as independent variables. The analysis was also repeated using ANCOVA on
650 Box-Cox transformed data. Both analyses revealed no significant statistical relationship
651 between N₂O flux and any of these environmental variables, with the exception of soil
652 temperature, which showed only a weak positive relationship to N₂O flux when the data was
653 analysed using the GLM ($P < 0.05$). This relationship was not detected using ANCOVA.

654 Bivariate regression of soil temperature against N₂O flux indicated that the relationship was
655 relatively weak, with $r^2 = 0.01$ ($P < 0.05$).

656

657 **5.6 Nitrate addition experiment**

658 ¹⁵N-N₂O and ¹⁵N-N₂ fluxes showed a biphasic response (Limmer and Steele, 1982), with
659 significantly different flux rates in the first 24 hours of incubation compared to the later
660 period of incubation (i.e. 24-48 hours). Flux of ¹⁵N-N₂O, and ¹⁵N-N₂ were therefore divided
661 into early (0-24 hours) and late (24-48 hours) phase flux.

662

663 **5.6.1 ¹⁵N-N₂O flux**

664 For the ¹⁵N-N₂O flux data, we used a full factorial ANOVA on Box-Cox transformed data with
665 habitat, N addition level, incubation phase, and all their interaction terms as independent
666 variables. Habitat, incubation phase, and the habitat by incubation phase interaction all
667 significantly influenced ¹⁵N-N₂O flux (ANOVA, $F_{29, 149} = 5.67$, $P < 0.0001$; Figure 5;
668 Supplementary Online Materials Table S3A). Notably, N addition level did not significantly
669 influence ¹⁵N-N₂O flux. Of the three main factors (i.e. habitat, N addition level, incubation
670 phase), habitat was the best predictor of ¹⁵N-N₂O flux, explaining a largest proportion of the
671 variance (Supplementary Online Materials Table S3A). Upper montane forest organic layer
672 soils showed the highest flux (238 ± 160 ng N₂O-¹⁵N g⁻¹ d⁻¹), lower montane (179 ± 48 ng
673 N₂O-¹⁵N g⁻¹ d⁻¹) and premontane (86 ± 16 ng N₂O-¹⁵N g⁻¹ d⁻¹) forest showed intermediate flux,
674 while montane grasslands (11 ± 4 ng N₂O-¹⁵N g⁻¹ d⁻¹) and upper montane forest mineral layer
675 soils (0.06 ± 0.01 ng N₂O-¹⁵N g⁻¹ d⁻¹) showed the lowest flux (Fisher's LSD, $P < 0.05$). The
676 effect of incubation phase was attributable to significantly greater ¹⁵N-N₂O flux during the
677 late compared to early incubation phases (164 ± 66 ng N₂O-¹⁵N g⁻¹ d⁻¹ versus 42 ± 11 ng N₂O-
678 ¹⁵N g⁻¹ d⁻¹; t-Test, $P < 0.05$; Figure 5). The habitat by incubation phase interaction was caused
679 by some habitats showing higher flux in certain incubation phases than others (Figure 5).
680 During the early phase, lower montane and premontane forests collectively showed the
681 highest flux (Figure 5; Fisher's LSD, $P < 0.05$). In contrast, during the late incubation phase,
682 upper montane forest organic layer soils, lower montane forest, and premontane forest now
683 showed the highest flux (Figure 5; Fisher's LSD, $P < 0.05$).

684

685 **5.6.2 ¹⁵N-N₂ flux**

686 For the $^{15}\text{N-N}_2$ flux data, we used a full factorial ANOVA on Box-Cox transformed data with
687 habitat, N addition level, incubation phase, and all their interaction terms as independent
688 variables. Only habitat significantly influenced flux, while other terms were not significant
689 (ANOVA, $F_{29, 149} = 1.66$, $P < 0.05$; Figure 5; Supplementary Online Materials Table S3B). Lower
690 montane and upper montane forest organic layer soils showed the highest flux (472 ± 139
691 and $576 \pm 117 \text{ ng N}_2\text{-}^{15}\text{N g}^{-1} \text{ d}^{-1}$, respectively), while all other habitats showed similar flux
692 rates ($105 \pm 19 \text{ ng N}_2\text{-}^{15}\text{N g}^{-1} \text{ d}^{-1}$) (Fisher's LSD, $P < 0.05$; Figure 5).

693

694 **5.6.3 N₂O Yield**

695 For the N₂O yield, we used a full factorial ANOVA on Box-Cox transformed data with habitat,
696 N addition level, incubation phase (i.e. early versus late), and all their interaction terms as
697 independent variables. We found that none of these factors predicted N₂O yield (ANOVA,
698 $F_{29, 149} = 0.75$, $P > 0.82$; Supplementary Online Materials Table S3C). The overall mean N₂O
699 yield for the pooled dataset was 0.53 ± 0.04 .

700

701

702 **6. Discussion**

703 **6.1 Effects of seasonality and soil moisture on N₂O flux**

704 Nitrous oxide flux in the Kosñipata Valley showed weak seasonality, with greater N₂O flux
705 during the dry season compared to the wet season. This regional trend was consistent with
706 results from our prior study, and was principally driven by strong seasonality in N₂O flux
707 from lower montane forest (Teh et al., 2014). In contrast, other habitats showed little or no
708 seasonal variation in N₂O flux. This weak seasonality in N₂O flux across the Kosñipata Valley
709 probably stems from relatively modest variation in environmental variables among seasons
710 (Table 3), in accordance with observations from elsewhere in the Andes (Baldos et al.,
711 2015;Müller et al., 2015;Wolf et al., 2011). For example, while soil moisture (i.e. WFPS)
712 varied significantly between seasons in the dataset as a whole, the absolute difference in
713 WFPS between dry season and wet season were relatively small (i.e. 7.4 %). Indeed, some
714 habitats showed much smaller variations in soil moisture, such as premontane forest and
715 montane grassland that showed no significant seasonal variation in WFPS whatsoever (Table
716 3).

717

718 One critical factor contributing to these weak seasonal trends in N₂O flux is the atypical
719 response of N₂O flux to changes in soil moisture. Nitrous oxide flux showed a weak but
720 negative correlation with WFPS in the field dataset ($r^2 = 0.01$, $P < 0.06$ for the pooled dataset),
721 rather than following a curvilinear pattern predicted by denitrification theory (Firestone and
722 Davidson, 1989; Firestone et al., 1980; Weier et al., 1993; Davidson, 1991). Likewise, in our soil
723 moisture manipulation experiments, nitrification made a minor contribution to N₂O
724 production, irrespective of soil moisture content (Supplementary Online Materials Figure
725 S1). This finding is contrary to theoretical predictions of N₂O production by ammonia-
726 oxidizing bacteria (AOB), where N₂O production from ammonia-oxidation is thought to make
727 an important contribution to N₂O flux at lower soil moisture contents (i.e. 30-60 % WFPS)
728 (Firestone and Davidson, 1989; Firestone et al., 1980; Weier et al., 1993; Davidson, 1991). At
729 higher soil moisture contents (i.e. >60 % WFPS), N₂O flux showed a non-linear response to
730 increasing WFPS, with two distinct peaks in N₂O flux at 90 and 50 % WFPS (Figure 4).
731 Collectively, these findings suggest that the role of soil moisture in regulating N₂O flux is
732 more complex than predicted by existing theory, falsifying our first two hypotheses.

733

734 What could explain these unexpected trends? We believe that these patterns occurred due
735 to the complex interplay between environmental conditions and the microbial processes
736 that produce N₂O in soil (i.e. ammonia oxidation by archaea, ammonia oxidation by bacteria,
737 denitrification, dissimilatory nitrate reduction to ammonium). We suspect that the action of
738 lesser-known microbial processes, such as oxidation of ammonia by archaea and
739 dissimilatory nitrate reduction to ammonium (DNRA), may explain the divergence from
740 theoretical norms. Our expectations of how N₂O production should respond to variations in
741 soil moisture are predicated on the assumption that N₂O is produced almost exclusively by
742 AOB and denitrifying bacteria, with the former operating at lower soil moisture content (i.e.
743 30-60 % WFPS) and the latter at higher soil moisture content (i.e. >60 % WFPS) (Firestone
744 and Davidson, 1989; Firestone et al., 1980; Weier et al., 1993; Davidson, 1991). More recent
745 advances in soil N research, however, have highlighted the importance of other microbial
746 taxa or processes, not previously considered in conceptual or process-based models. For
747 example, recent work in acidic soils have demonstrated that ammonia oxidizing archaea
748 (AOA) play a more important role than AOB in ammonia oxidation, but produce significantly
749 less N₂O due to differences in metabolism (Hink et al., 2016; Prosser and Nicol, 2008).

750 Likewise, under higher soil moisture conditions (>60 % WFPS), DNRA – a process that
751 produces substantially less N₂O than denitrification and which also competes for NO₃⁻ with
752 denitrification – can dominate nitrate reduction, depending on redox conditions and the
753 relative availability of labile C and N (Morley and Baggs, 2010;Pett-Ridge and Firestone,
754 2005;Silver et al., 2001;Baldos et al., 2015;Müller et al., 2015). Thus, given the low pH of the
755 soils in Kosñipata Valley (Table 1), it is likely that AOA dominate ammonia oxidation at lower
756 levels of soil moisture, explaining the negligible amounts of N₂O produced from nitrification
757 in the 30 and 50 % WFPS treatments. As soils become wetter, the non-linear response of
758 N₂O flux to increasing soil moisture may reflect competition for substrates (e.g. NO₃⁻,
759 reducing equivalents) between DNRA and denitrification (Morley and Baggs, 2010;Silver et
760 al., 2001), or may indicate that DNRA is making a larger contribution to N₂O flux than
761 denitrification (Streminska et al., 2012).

762

763 These findings are important and noteworthy, given that climatically-driven variations in soil
764 moisture content are thought to be one of the dominant drivers for N₂O flux in the
765 seasonally dry tropics (Davidson, 1991;Firestone and Davidson, 1989;Groffman et al.,
766 2009;Davidson and Verchot, 2000;Teh et al., 2014;van Lent et al., 2015;Werner et al., 2007).
767 Moreover, similar results from comparable research sites in the Ecuadorian Andes lend
768 credence to our claims (Baldos et al., 2015;Müller et al., 2015). For example, Müller et al.
769 (2015) found that nitrification produced little or no N₂O in acidic Ecuadorian soils, in
770 agreement with findings from in this study. Likewise, ¹⁵N isotope pool dilution experiments,
771 in comparable habitats and elevations to our own, revealed that DNRA played a significant
772 role in nitrate reduction, supporting the notion that DNRA may represent a substantial sink
773 for NO₃⁻ in Peruvian soils (Baldos et al., 2015;Müller et al., 2015). Existing process-based
774 models, which are used to construct bottom-up emissions inventories for the tropics
775 (Werner et al., 2007), often assume that N₂O is derived primarily from AOB and
776 denitrification, with moisture response curves based on existing theoretical relationships (Li
777 et al., 2000;Werner et al., 2007;Smith et al., 2007). However, if these more “normative” soil
778 moisture response curves are inapplicable to montane tropical ecosystems, due to the
779 activity of AOA and DNRA, then a re-conceptualisation of the soil moisture-N₂O flux
780 relationship may be required. Moreover, if weak seasonality or aseasonality in N₂O flux is
781 the norm in Andean ecosystems (Müller et al., 2015;Wolf et al., 2011), then this finding may

782 have wider implications for understanding spatial or temporal trends in regional
783 atmospheric budgets (Kort et al., 2011; Nevison et al., 2004; Nevison et al., 2007; Saikawa et
784 al., 2014).

785

786 **6.2 Role of substrate limitation in regulating N₂O flux**

787 In accordance with our earlier work (Teh et al., 2014) and research conducted in analogous
788 ecosystems in Ecuador (Baldos et al., 2015; Müller et al., 2015; Wolf et al., 2011), we found
789 strong evidence that N₂O flux was constrained by the availability of NO₃⁻, partially supporting
790 our third hypothesis. In contrast, N₂O flux was unresponsive to short-term changes in labile
791 organic matter (i.e. leaf litter-fall) inputs, indicating that N₂O flux and nitrate reduction were
792 not C limited. This latter result is significant for modelling and extrapolating N₂O flux from
793 these habitats, because many process-based models assume that N cycling and turnover of
794 labile organic matter are intimately linked through processes such as litter production and
795 decomposition (Li et al., 2000; Werner et al., 2007; Smith et al., 2007).

796

797 Evidence for NO₃⁻ limitation of N₂O flux comes from both our field and laboratory data, and
798 suggests that “habitat” may be a good proxy for NO₃⁻ availability and N₂O flux because these
799 two variables co-vary with habitat. For example, we observed an inverse trend in field N₂O
800 flux, with premontane forest showing significantly greater flux than the other habitats
801 elevation (Table 3, Figure 2a). This inverse trend was also reflected in the resin-extractable
802 NO₃⁻ flux measured in the field and the ¹⁵N-N₂O flux measured in the NO₃⁻ addition
803 experiment in the laboratory (Figure 2c, 5a). Furthermore, the behaviour of the ¹⁵N-NO₃⁻
804 amended soils during the early (≤24 hours) and late (>24 hours) phases of the incubation
805 experiment suggest that soils from more N-poor habitats (i.e. those with lower rates of
806 resin-extractable NO₃⁻ flux; Table 3, Figure 2c) showed a greater proportional increase in ¹⁵N-
807 N₂O flux following NO₃⁻ addition than N-rich habitats (i.e. those with higher rates of resin-
808 extractable NO₃⁻ flux; Table 3, Figure 2c), suggesting that ¹⁵N-N₂O flux was more NO₃⁻ limited
809 in N-poor soils (Figure 5). Soils from the upper montane forest organic layer, montane
810 grasslands, and upper montane forest mineral layer showed the lowest ¹⁵N-N₂O flux during
811 the early phase of soil incubation, but the greatest proportional increase in flux during the
812 late phase of soil incubation, rising by a factor of 59, five, and two, respectively. In contrast,
813 lower montane and premontane forest soils showed the smallest proportional increase in

814 the late phase of soil incubation (i.e. 1.7 times increase). Last, the relatively low N₂O yield
815 observed in our soil moisture manipulations is thought to be broadly indicative of low NO₃⁻
816 conditions (i.e. <0.42 for forested habitats; Table 4), further supporting the notion that N₂O
817 flux in this region is generally NO₃⁻ limited (Schlesinger, 2009; Fang et al., 2015; Weier et al.,
818 1993).

819
820 Interestingly, increasing NO₃⁻ availability *per se* did not stimulate ¹⁵N-N₂O flux, ¹⁵N-N₂ flux, or
821 alter N₂O yield during the early phase (<24 hours) of the NO₃⁻ addition experiment, even
822 though we did observe that ¹⁵N-N₂O flux did increase during the late phase (>24 hours) of
823 the experiments (please see Figure 5 and discussion in the preceding paragraph). Rather,
824 ANCOVA suggests that ¹⁵N-N₂O and ¹⁵N-N₂ fluxes in the early phase of the NO₃⁻ addition
825 experiment were better-predicted by habitat; i.e. that soil provenance was a better
826 predictor of ¹⁵N-N₂O flux than N treatment). N₂O yield, normally a sensitive indicator of NO₃⁻
827 availability (Blackmer and Bremner, 1978; Weier et al., 1993; Parton et al., 1996), also showed
828 no immediate response to the amount of ¹⁵N-NO₃⁻ added, nor any of the other explanatory
829 variables. One explanation for this, consistent with the notion that N₂O flux is NO₃⁻ limited, is
830 that nitrate-reducing microbes in these soils may have a relatively low half-saturation
831 constant (K_m) for NO₃⁻, and effectively utilize NO₃⁻ whenever concentrations increase above
832 baseline (i.e. non-limiting) levels (Holtan-Hartwig et al., 2000). As a consequence, we may be
833 unable to differentiate among NO₃⁻ treatments in the early phase of the experiment,
834 because the amount of NO₃⁻ added exceeded the K_m for these soils. This finding is also in
835 agreement with results from long-term N fertilization studies, which suggest that
836 substantive shifts in N₂O flux are only likely to occur after prolonged exposure to high levels
837 of N (i.e. >1 year), rather than due to transient fluctuations in N availability (Baldos et al.,
838 2015; Corre et al., 2010; Müller et al., 2015; Hall and Matson, 1999; Koehler et al., 2012).

839

840 **6.3 Implications for annual atmospheric budgets and gaseous N loss**

841 Montane ecosystems in the Kosñipata Valley were net sources of atmospheric N₂O, affirming
842 our prior results (Teh et al., 2014). The flux for this multi-annual dataset was comparable to
843 the preliminary values reported in our earlier publication, with an unweighted mean flux of
844 0.27 ± 0.07 mg N-N₂O m⁻² d⁻¹ observed over a 30 month period compared to 0.22 ± 0.12 mg
845 N-N₂O m⁻² d⁻¹ recorded over a 13 month period (Teh et al., 2014). These values correspond

846 to unweighted mean annual fluxes of 0.99 ± 0.26 kg N₂O-N ha⁻¹ year⁻¹ and 0.80 ± 0.44 kg
847 N₂O-N ha⁻¹ year⁻¹, respectively. However, in order to derive more accurate estimates of the
848 annual contribution of the Kosñipata Valley to the regional atmospheric budget of N₂O, it is
849 necessary to account for differences in land area for different habitats and variation in the
850 magnitude of N₂O flux between seasons. Thus, we conducted a simple weighted upscaling
851 exercise to more fully account for these two sources of variation (Table 4). Using the N₂O
852 yield data from the laboratory tracer experiments, we also estimated the annual N₂ flux and
853 total gaseous N flux, in order compare rates of gaseous N export from this region with other
854 forested ecosystems (Fang et al., 2015; Russell and Raich, 2012; Tietema and Verstraten,
855 1991; Bai et al., 2012) (Table 4). We fully acknowledge that this simple approach is not as
856 robust as bottom-up, process-based emissions inventories (Werner et al., 2007). Even so, we
857 believe it is still useful for providing first-order approximations of annual N₂O, N₂ and total
858 gaseous N flux.

859

860 To briefly summarize our methodology, our first step was to use published surface area
861 estimates for the different habitats in the Kosñipata Valley to derive areal fractions for each
862 habitat (Feeley and Silman, 2010) (Table 4). Next, we multiplied the unweighted seasonal
863 mean flux by the areal fraction for each habitat to derive area-weighted seasonal flux
864 estimates (Table 4). We subsequently multiplied the area-weighted seasonal flux by the
865 fraction of the year accounted for by either season, in order to produce an area-weighted
866 and seasonally-weighted annual flux estimate for each habitat (Table 4). The final step of this
867 process was to sum the area-weighted and seasonally-weighted flux estimates for each
868 habitat, to drive an overall weighted flux estimate for the Kosñipata Valley as a whole (Table
869 4). Weighted annual estimates of N₂ flux were calculated using the N₂O yield values for each
870 habitat as determined in our soil moisture manipulation experiment (Table 4). We elected to
871 use mean N₂O yields for each habitat, rather than estimating N₂O yield based on soil
872 moisture content, because ANCOVA indicated that habitat was a better predictor of N₂O
873 yield than soil moisture, explaining a substantially greater proportion of the variance (i.e. 10
874 % versus only 1 % of the variance; see Supplementary Online Materials Table S2C). Total
875 gaseous N export was estimate by calculating the sum of annual N₂O and N₂ flux. Errors for
876 all the annual flux estimates (i.e. N₂O, N₂, total gaseous N) were propagated using standard
877 error propagation techniques.

878

879 We determined that the Kosñipata Valley emitted approximately $1.27 \pm 0.33 \text{ kg N}_2\text{O-N ha}^{-1}$
880 year^{-1} , $3.29 \pm 1.27 \text{ kg N}_2\text{-N ha}^{-1} \text{ year}^{-1}$, and $4.57 \pm 1.31 \text{ kg N ha}^{-1} \text{ year}^{-1}$. Annual N_2O flux was
881 broadly on par with our earlier estimates (i.e. $1.18 \pm 0.79 \text{ kg N}_2\text{O-N ha}^{-1} \text{ year}^{-1}$) (Teh et al.,
882 2014). This estimated annual rate of flux exceeds the value for montane tropical montane
883 forests calculated by Werner et al. (2007) using a bottom-up process model (i.e. 0.5 to 1 kg
884 $\text{N}_2\text{O-N ha}^{-1} \text{ year}^{-1}$), but falls within the range predicted for humid tropical forest soils more
885 generally (i.e. approximately 1-4 kg $\text{N}_2\text{O-N ha}^{-1} \text{ year}^{-1}$) (van Lent et al., 2015; Werner et al.,
886 2007). Annual N_2 flux and total gaseous N flux are at the lower end of the range reported in
887 comparable studies from other ecosystems (e.g. Fang et al., 2015 reported annual gaseous
888 losses of 5.6– 30.1 kg N $\text{ha}^{-1} \text{ year}^{-1}$ sampling across a broad range of temperate and tropical
889 ecosystems) (Fang et al., 2015; Russell and Raich, 2012; Tietema and Verstraten, 1991; Bai et
890 al., 2012), further supporting claims that Andean ecosystems are relatively N limited, and
891 may cycle N more conservatively than lowland forests (Baldos et al., 2015; Müller et al.,
892 2015; Wolf et al., 2011; Nottingham et al., 2015)

893

894

895 **7. Conclusions**

896 Process-based studies of N_2O flux from montane tropical ecosystems in the southern
897 Peruvian Andes affirms prior research suggesting that these ecosystems are potentially
898 important regional sources of N_2O (Teh et al., 2014). Simple weighted upscaling suggests
899 that annual N_2O flux from the Kosñipata Valley is on the order of $1.27 \pm 0.33 \text{ kg N}_2\text{O-N ha}^{-1}$.
900 Habitat – a proxy for NO_3^- availability under field conditions – was the best predictor for N_2O
901 flux, with more N-rich habitats (i.e. premontane forest) showing significantly higher N_2O flux
902 than habitats with lower N availability (i.e. upper montane forest, montane grassland).
903 Nitrous oxide flux originated primarily from nitrate reduction rather than from nitrification,
904 probably due to low pH soil conditions which may have inhibited the activity of AOB.
905 Contrary to our prior research, we found only weak evidence for seasonal trends in field N_2O
906 flux, with the exception of lower montane forest, which showed significantly higher N_2O flux
907 during the dry season compared to the wet season. Weak seasonal trends in field N_2O flux
908 among the other montane habitats probably stems from relatively modest seasonal
909 variation in key environmental drivers (e.g. temperature, WFPS, NO_3^-), combined with a soil

910 moisture response that was complex and non-linear. Nitrous oxide flux was significantly
911 influenced by soil moisture content, but the trends in N₂O production and flux diverged from
912 theoretical norms. For example, we saw little evidence of N₂O production from ammonia-
913 oxidation, even though the field measurement (i.e. resin bags) indicate that nitrification
914 occurs. This may be due to the predominance of AOA, which produce significantly N₂O than
915 AOB, under the acidic conditions common in Andean soils. At higher soil moisture levels, N₂O
916 flux increased non-linearly with WFPS, with peaks in N₂O flux at 90 and 50 % WFPS. These
917 results suggest that the effects of water on N₂O flux are complicated by other factors, such
918 as competition for substrates among different nitrate-reducing processes, or shifts in the
919 amount of N₂O derived from denitrification or DNRA. Field data and substrate manipulation
920 experiments indicated that N₂O flux was strongly limited by NO₃⁻, but unconstrained by the
921 input rate of labile organic matter (i.e. leaf litter). Nitrous oxide flux was relatively insensitive
922 to short-term variations in NO₃⁻, and was better-predicted by longer-term, time-averaged
923 variations in NO₃⁻ availability.

924

925

926 **8. Data Availability**

927 Data for this publication are publically available from the UK Natural Environment Research
928 Council (NERC) Centre for Environmental Data Analysis (CEDA), at the following URL:

929 <http://catalogue.ceda.ac.uk/uuid/93fdb48b713b4dbc93a28d695771312d>

930

931

932 **9. Author Contributions**

933 TD designed the field and laboratory experiments, collected the field data, conducted the
934 laboratory experiments, processed the samples, analysed the data, and contributed to the
935 preparation of the manuscript. NJM contributed to the design of the laboratory
936 experiments, assisted in the sample analysis, assisted in the analysis of the laboratory data,
937 and contributed to the preparation of the manuscript. AJC and LPHQ assisted in the
938 collection of the field data and processing of the field samples. EMB, PM, MR, and PS
939 contributed to the experimental design and the preparation of the manuscript. YAT directed
940 the research, contributed to the design of the experiments, assisted in the analysis of the
941 field and laboratory data, and took the principal role in preparing the manuscript.

942

943

944 **10. Acknowledgements**

945 The authors would like to acknowledge the agencies that funded this research; the UK
946 Natural Environment Research Council (NERC; joint grant references NE/H006583,
947 NE/H007849 and NE/H006753). Patrick Meir was supported by an Australian Research
948 Council Fellowship (FT110100457). Javier Eduardo Silva Espejo, Walter Huaraca Huasco, and
949 the ABIDA NGO provided critical fieldwork and logistical support. Angus Calder (University of
950 St Andrews) and Vicky Munro (University of Aberdeen) provided invaluable laboratory
951 support. Thanks to Adrian Tejedor from the Amazon Conservation Association, who provided
952 assistance with site access and site selection at Hacienda Villa Carmen. This publication is a
953 contribution from the Scottish Alliance for Geoscience, Environment and Society
954 (<http://www.sages.ac.uk>).

955

956

957 **11. References**

958 Baggs, E. M., Richter, M., Hartwig, U.A., and Cadisch, G. : Nitrous oxide emissions from grass
959 swards during the eighth year of elevated atmospheric pCO₂ (Swiss FACE). , *Global Change*
960 *Biology* 9, 1214-1222., 2003.

961 Bai, E., Houlton, B. Z., and Wang, Y. P.: Isotopic identification of nitrogen hotspots across
962 natural terrestrial ecosystems, *Biogeosciences*, 9, 3287-3304, 10.5194/bg-9-3287-2012,
963 2012.

964 Baldos, A. P., Corre, M. D., and Veldkamp, E.: Response of N cycling to nutrient inputs in
965 forest soils across a 1000–3000 m elevation gradient in the Ecuadorian Andes, *Ecology*, 96,
966 749-761, 10.1890/14-0295.1, 2015.

967 Bateman, E. J., and Baggs, E. M.: Contributions of nitrification and denitrification to N₂O
968 emissions from soils at different water-filled pore space, *Biology and Fertility of Soils*, 41,
969 379-388, 10.1007/s00374-005-0858-3, 2005.

970 Belyea, L. R., and Baird, A. J.: Beyond "The limits to peat bog growth": Cross-scale feedback
971 in peatland development, *Ecological Monographs*, 76, 299-322, 2006.

972 Blackmer, A. M., and Bremner, J. M.: Inhibitory effect of nitrate on reduction of N₂O to N₂
973 by soil microorganisms, *Soil Biology and Biochemistry*, 10, 187-191,
974 [http://dx.doi.org/10.1016/0038-0717\(78\)90095-0](http://dx.doi.org/10.1016/0038-0717(78)90095-0), 1978.

975 Breuer, L., Papen, H., and Butterbach-Bahl, K.: N₂O emission from tropical forest soils of
976 Australia, *J. Geophys. Res.-Atmos.*, 105, 26353-26367, 10.1029/2000jd900424, 2000.

977 Corre, M. D., Veldkamp, E., Arnold, J., and Wright, S. J.: Impact of elevated N input on soil N
978 cycling and losses in old-growth lowland and montane forests in Panama, *Ecology*, 91, 1715-
979 1729, 10.1890/09-0274.1, 2010.

980 Davidson, E. A.: Fluxes of nitrous oxide and nitric oxide from terrestrial ecosystems, in:
981 *Microbial production and consumption of greenhouse gases: methane, nitrogen oxides, and*
982 *halomethanes.*, edited by: Rogers, J. E., and Whitman, W. B., American Society for
983 Microbiology, Washington D.C., 219-236, 1991.

984 Davidson, E. A., and Verchot, L. V.: Testing the Hole-in-the-Pipe Model of nitric and nitrous
985 oxide emissions from soils using the TRAGNET Database, *Global Biogeochemical Cycles*, 14,
986 1035-1043, 10.1029/1999GB001223, 2000.

987 Eva, H. D., Belward, A. S., De Miranda, E. E., Di Bella, C. M., Gond, V., Huber, O., Jones, S.,
988 Sgrenzaroli, M., and Fritz, S.: A land cover map of South America, *Global Change Biology*, 10,
989 731-744, 10.1111/j.1529-8817.2003.00774.x, 2004.

990 Fang, Y., Koba, K., Makabe, A., Takahashi, C., Zhu, W., Hayashi, T., Hokari, A. A., Urakawa, R.,
991 Bai, E., Houlton, B. Z., Xi, D., Zhang, S., Matsushita, K., Tu, Y., Liu, D., Zhu, F., Wang, Z., Zhou,
992 G., Chen, D., Makita, T., Toda, H., Liu, X., Chen, Q., Zhang, D., Li, Y., and Yoh, M.: Microbial
993 denitrification dominates nitrate losses from forest ecosystems, *Proceedings of the National*
994 *Academy of Sciences*, 112, 1470-1474, 10.1073/pnas.1416776112, 2015.

995 Feeley, K. J., and Silman, M. R.: Land-use and climate change effects on population size and
996 extinction risk of Andean plants, *Global Change Biology*, 16, 3215-3222, 10.1111/j.1365-
997 2486.2010.02197.x, 2010.

998 Firestone, M. K., Firestone, R. B., and Tiedje, J. M.: Nitrous oxide from soil denitrification:
999 Factors controlling its biological production., *Science*, 208, 749-751, 1980.

1000 Firestone, M. K., and Davidson, E. A.: Microbiological basis of NO and N₂O production and
1001 consumption in soil, in: *Exchange of Trace Gases Between Terrestrial Ecosystems and the*
1002 *Atmosphere*, edited by: Andrae, M. O., and Schimel, D. S., John Wiley and Sons Ltd., New
1003 York, 7-21, 1989.

1004 Girardin, C. A. J., Malhi, Y., Aragão, L. E. O. C., Mamani, M., Huaraca Huasco, W., Durand, L.,
1005 Feeley, K. J., Rapp, J., Silva-Espejo, J. E., Silman, M., Salinas, N., and Whittaker, R. J.: Net
1006 primary productivity allocation and cycling of carbon along a tropical forest elevational
1007 transect in the Peruvian Andes, *Global Change Biology*, 16, 3176-3192, 10.1111/j.1365-
1008 2486.2010.02235.x, 2010.

1009 Groffman, P. M., Butterbach-Bahl, K., Fulweiler, R. W., Gold, A. J., Morse, J. L., Stander, E. K.,
1010 Tague, C., Tonitto, C., and Vidon, P.: Challenges to incorporating spatially and temporally
1011 explicit phenomena (hotspots and hot moments) in denitrification models, *Biogeochemistry*,
1012 93, 49-77, 10.1007/s10533-008-9277-5, 2009.

1013 Hall, S. J., and Matson, P. A.: Nitrogen oxide emissions after nitrogen additions in tropical
1014 forests, *Nature*, 400, 152-155, 1999.

1015 Hink, L., Nicol, G. W., and Prosser, J. I.: Archaea produce lower yields of N₂O than bacteria
1016 during aerobic ammonia oxidation in soil, *Environ. Microbiol.*, n/a-n/a, 10.1111/1462-
1017 2920.13282, 2016.

1018 Hirsch, A. I., Michalak, A. M., Bruhwiler, L. M., Peters, W., Dlugokencky, E. J., and Tans, P. P.:
1019 Inverse modeling estimates of the global nitrous oxide surface flux from 1998-2001, *Global*
1020 *Biogeochemical Cycles*, 20, 1-17, Gb1008
1021 10.1029/2004gb002443, 2006.

1022 Holtan-Hartwig, L., Dorsch, P., and Bakken, L. R.: Comparison of denitrifying communities in
1023 organic soils: kinetics of NO₃⁻ and N₂O reduction, *Soil Biol. Biochem.*, 32, 833-843,
1024 10.1016/s0038-0717(99)00213-8, 2000.

1025 Huang, J., Golombek, A., Prinn, R., Weiss, R., Fraser, P., Simmonds, P., Dlugokencky, E. J.,
1026 Hall, B., Elkins, J., Steele, P., Langenfelds, R., Krummel, P., Dutton, G., and Porter, L.:
1027 Estimation of regional emissions of nitrous oxide from 1997 to 2005 using multinet
1028 measurements, a chemical transport model, and an inverse method, *J. Geophys. Res.-*
1029 *Atmos.*, 113, 1-19, D17313
1030 10.1029/2007jd009381, 2008.

1031 Jones, S. P., Diem, T., Huaraca Quispe, L. P., Cahuana, A. J., Reay, D. S., Meir, P., and Teh, Y.
1032 A.: Drivers of atmospheric methane uptake by montane forest soils in the southern Peruvian
1033 Andes, *Biogeosciences*, 13, 4151-4165, 10.5194/bg-13-4151-2016, 2016.

1034 Koehler, B., Corre, M. D., Steger, K., Well, R., Zehe, E., Sueta, J. P., and Veldkamp, E.: An in-
1035 depth look into a tropical lowland forest soil: nitrogen-addition effects on the contents of

1036 N₂O, CO₂ and CH₄ and N₂O isotopic signatures down to 2-m depth, *Biogeochemistry*, 111,
1037 695-713, 10.1007/s10533-012-9711-6, 2012.

1038 Kort, E. A., Patra, P. K., Ishijima, K., Daube, B. C., Jimenez, R., Elkins, J., Hurst, D., Moore, F. L.,
1039 Sweeney, C., and Wofsy, S. C.: Tropospheric distribution and variability of N₂O: Evidence for
1040 strong tropical emissions, *Geophys. Res. Lett.*, 38, 5, 10.1029/2011gl047612, 2011.

1041 Li, C., Aber, J., Stange, F., Butterbach-Bahl, K., and Papen, H.: A process-oriented model of
1042 N₂O and NO emissions from forest soils: 1. Model development, *Journal of Geophysical*
1043 *Research: Atmospheres*, 105, 4369-4384, 10.1029/1999JD900949, 2000.

1044 Limmer, A. W., and Steele, K. W.: Denitrification potentials: Measurement of seasonal
1045 variation using a short-term anaerobic incubation technique, *Soil Biology and Biochemistry*,
1046 14, 179-184, [http://dx.doi.org/10.1016/0038-0717\(82\)90020-7](http://dx.doi.org/10.1016/0038-0717(82)90020-7), 1982.

1047 Livingston, G., and Hutchinson, G.: Chapter 2: Enclosure-based measurement of trace gas
1048 exchange: applications and sources of error., in: *Biogenic Trace Gases: Measuring Emissions*
1049 *from Soil and Water.*, edited by: Matson, P., Harriss, RC, Blackwell Science Ltd, Cambridge,
1050 MA, USA, 14-51, 1995.

1051 Malhi, Y., Silman, M., Salinas, N., Bush, M., Meir, P., and Saatchi, S.: Introduction: Elevation
1052 gradients in the tropics: laboratories for ecosystem ecology and global change research,
1053 *Global Change Biology*, 16, 3171-3175, 10.1111/j.1365-2486.2010.02323.x, 2010.

1054 Morley, N., and Baggs, E. M.: Carbon and oxygen controls on N₂O and N₂ production during
1055 nitrate reduction, *Soil Biol. Biochem.*, 42, 1864-1871, 10.1016/j.soilbio.2010.07.008, 2010.

1056 Moser, G., Leuschner, C., Hertel, D., Graefe, S., Soethe, N., and Iost, S.: Elevation effects on
1057 the carbon budget of tropical mountain forests (S Ecuador): the role of the belowground
1058 compartment, *Global Change Biology*, 17, 2211-2226, 10.1111/j.1365-2486.2010.02367.x,
1059 2011.

1060 Müller, A. K., Matson, A. L., Corre, M. D., and Veldkamp, E.: Soil N₂O fluxes along an
1061 elevation gradient of tropical montane forests under experimental nitrogen and phosphorus
1062 addition, *Frontiers in Earth Science*, 3, 66, 2015.

1063 Nevison, C. D., Lueker, T. J., and Weiss, R. F.: Quantifying the nitrous oxide source from
1064 coastal upwelling, *Global Biogeochemical Cycles*, 18, 24, Gb1018
1065 10.1029/2003gb002110, 2004.

1066 Nevison, C. D., Mahowald, N. M., Weiss, R. F., and Prinn, R. G.: Interannual and seasonal
1067 variability in atmospheric N₂O, *Global Biogeochemical Cycles*, 21, GB3017,
1068 10.1029/2006GB002755, 2007.

1069 Nottingham, A. T., Turner, B. L., Whitaker, J., Ostle, N. J., McNamara, N. P., Bardgett, R. D.,
1070 Salinas, N., and Meir, P.: Soil microbial nutrient constraints along a tropical forest elevation
1071 gradient: a belowground test of a biogeochemical paradigm, *Biogeosciences*, 12, 6071-6083,
1072 10.5194/bg-12-6071-2015, 2015.

1073 Parton, W. J., Mosier, A. R., Ojima, D. S., Valentine, D. W., Schimel, D. S., Weier, K., and
1074 Kulmala, A. E.: Generalized model for N₂ and N₂O production from nitrification and
1075 denitrification, *Global Biogeochemical Cycles*, 10, 401-412, 10.1029/96GB01455, 1996.

1076 Pedersen, A. R., Petersen, S. O., and Schelde, K.: A comprehensive approach to soil-
1077 atmosphere trace-gas flux estimation with static chambers, *European Journal of Soil Science*,
1078 61, 888-902, 10.1111/j.1365-2389.2010.01291.x, 2010.

1079 Pett-Ridge, J., and Firestone, M. K.: Redox fluctuation structures microbial communities in a
1080 wet tropical soil, *Appl. Environ. Microbiol.*, 71, 6998-7007, 10.1128/aem.71.11.6998-
1081 7007.2005, 2005.

1082 Potter, C. S., Matson, P. A., Vitousek, P. M., and Davidson, E. A.: Process modeling of controls
1083 on nitrogen trace gas emissions from soils worldwide, *Journal of Geophysical Research:*
1084 *Atmospheres*, 101, 1361-1377, 10.1029/95JD02028, 1996.

1085 Prosser, J. I., and Nicol, G. W.: Relative contributions of archaea and bacteria to aerobic
1086 ammonia oxidation in the environment, *Environ. Microbiol.*, 10, 2931-2941, 10.1111/j.1462-
1087 2920.2008.01775.x, 2008.

1088 Pumpanen, J., Kolari, P., Ilvesniemi, H., Minkkinen, K., Vesala, T., Niinistö, S., Lohila, A.,
1089 Larmola, T., Morero, M., Pihlatie, M., Janssens, I., Yuste, J. C., Grünzweig, J. M., Reth, S.,
1090 Subke, J.-A., Savage, K., Kutsch, W., Østreg, G., Ziegler, W., Anthoni, P., Lindroth, A., and
1091 Hari, P.: Comparison of different chamber techniques for measuring soil CO₂ efflux, *Agric.*
1092 *For. Meteorol.*, 123, 159-176, <http://dx.doi.org/10.1016/j.agrformet.2003.12.001>, 2004.

1093 Russell, A. E., and Raich, J. W.: Rapidly growing tropical trees mobilize remarkable amounts
1094 of nitrogen, in ways that differ surprisingly among species, *Proceedings of the National*
1095 *Academy of Sciences*, 109, 10398-10402, 10.1073/pnas.1204157109, 2012.

1096 Saikawa, E., Schlosser, C. A., and Prinn, R. G.: Global modeling of soil nitrous oxide emissions
1097 from natural processes, *Global Biogeochemical Cycles*, 27, 972-989, 10.1002/gbc.20087,
1098 2013.

1099 Saikawa, E., Prinn, R. G., Dlugokencky, E., Ishijima, K., Dutton, G. S., Hall, B. D., Langenfelds,
1100 R., Tohjima, Y., Machida, T., Manizza, M., Rigby, M., O'Doherty, S., Patra, P. K., Harth, C. M.,
1101 Weiss, R. F., Krummel, P. B., van der Schoot, M., Fraser, P. J., Steele, L. P., Aoki, S., Nakazawa,
1102 T., and Elkins, J. W.: Global and regional emissions estimates for N₂O, *Atmospheric
1103 Chemistry and Physics*, 14, 4617-4641, 10.5194/acp-14-4617-2014, 2014.

1104 Schlesinger, W. H.: On the fate of anthropogenic nitrogen, *Proceedings of the National
1105 Academy of Sciences*, 106, 203-208, 10.1073/pnas.0810193105, 2009.

1106 Silver, W. L., Herman, D. J., and Firestone, M. K. S.: Dissimilatory Nitrate Reduction to
1107 Ammonium in Upland Tropical Forest Soils., *Ecology*, 82, 2410-2416, 2001.

1108 Smith, P., Smith, J. U., Flynn, H., Killham, K., Rangel-Castro, I., Foereid, B., Aitkenhead, M.,
1109 Chapman, S., Towers, W., Bell, J., Lumsdon, D., Milne, R., Thomson, A., Simmons, I., Skiba, U.,
1110 Reynolds, B., Evans, C., Frogbrook, Z., Bradley, I., Whitmore, A., and Falloon, P.: ECOSSE:
1111 Estimating Carbon in Organic Soils - Sequestration and Emissions. Final Report., Scottish
1112 Executive Environment and Rural Affairs Department Report, 166 pp., 2007.

1113 Streminska, M. A., Felgate, H., Rowley, G., Richardson, D. J., and Baggs, E. M.: Nitrous oxide
1114 production in soil isolates of nitrate-ammonifying bacteria, *Environ. Microbiol. Rep.*, 4, 66-
1115 71, 10.1111/j.1758-2229.2011.00302.x, 2012.

1116 Subler, S., Blair, J. M., and Edwards, C. A.: Using anion-exchange membranes to measure soil
1117 nitrate availability and net nitrification, *Soil Biology and Biochemistry*, 27, 911-917,
1118 [http://dx.doi.org/10.1016/0038-0717\(95\)00008-3](http://dx.doi.org/10.1016/0038-0717(95)00008-3), 1995.

1119 Team, R. C.: A language and environment for statistical computing, R Foundation for
1120 Statistical Computing, Vienna, Austria, 2012.

1121 Teh, Y. A., Diem, T., Jones, S., Huaraca Quispe, L. P., Baggs, E., Morley, N., Richards, M.,
1122 Smith, P., and Meir, P.: Methane and nitrous oxide fluxes across an elevation gradient in the
1123 tropical Peruvian Andes, *Biogeosciences*, 11, 2325-2339, 10.5194/bg-11-2325-2014, 2014.

1124 Templer, P. H., Lovett, G. M., Weathers, K. C., Findlay, S. E., and Dawson, T. E.: Influence of
1125 tree species on forest nitrogen retention in the Catskill Mountains, New York, USA,
1126 *Ecosystems*, 8, 1-16, 10.1007/s10021-004-0230-8, 2005.

1127 Tietema, A., and Verstraten, J. M.: Nitrogen cycling in an acid forest ecosystem in the
1128 Netherlands under increased atmospheric nitrogen input, *Biogeochemistry*, 15, 21-46,
1129 10.1007/bf00002807, 1991.

1130 van Lent, J., Hergoualc'h, K., and Verchot, L. V.: Reviews and syntheses: Soil N₂O and NO
1131 emissions from land use and land use change in the tropics and subtropics: a meta-analysis,
1132 *Biogeosciences*, 15, 7299-7313 pp., 2015.

1133 Varner, R. K., Keller, M., Robertson, J. R., Dias, J. D., Silva, H., Crill, P. M., McGroddy, M., and
1134 Silver, W. L.: Experimentally induced root mortality increased nitrous oxide emission from
1135 tropical forest soils, *Geophys. Res. Lett.*, 30, n/a-n/a, 10.1029/2002GL016164, 2003.

1136 Veldkamp, E., Purbopuspito, J., Corre, M. D., Brumme, R., and Murdiyarso, D.: Land use
1137 change effects on trace gas fluxes in the forest margins of Central Sulawesi, Indonesia,
1138 *Journal of Geophysical Research-Biogeosciences*, 113, 1-11, G02003
1139 10.1029/2007jg000522, 2008.

1140 Weier, K. L., Doran, J. W., Power, J. F., and Walters, D. T.: Denitrification and the denitrogen
1141 nitrous oxide ratio as affected by soil water, available carbon, and nitrate, *Soil Sci. Soc. Am.*
1142 *J.*, 57, 66-72, 1993.

1143 Werner, C., Butterbach-Bahl, K., Haas, E., Hickler, T., and Kiese, R.: A global inventory of N₂O
1144 emissions from tropical rainforest soils using a detailed biogeochemical model, *Global*
1145 *Biogeochemical Cycles*, 21, 1-18, Gb3010
1146 10.1029/2006gb002909, 2007.

1147 Wolf, K., Veldkamp, E., Homeier, J., and Martinson, G. O.: Nitrogen availability links forest
1148 productivity, soil nitrous oxide and nitric oxide fluxes of a tropical montane forest in
1149 southern Ecuador, *Global Biogeochemical Cycles*, 25, GB4009, 10.1029/2010GB003876,
1150 2011.

1151 Wolf, K., Flessa, H., and Veldkamp, E.: Atmospheric methane uptake by tropical montane
1152 forest soils and the contribution of organic layers, *Biogeochemistry*, 111, 469-483,
1153 10.1007/s10533-011-9681-0, 2012.

1154 Zimmermann, M., Meir, P., Bird, M., Malhi, Y., and Ccahuana, A.: Litter contribution to
1155 diurnal and annual soil respiration in a tropical montane cloud forest, *Soil Biology and*
1156 *Biochemistry*, 41, 1338-1340, 2009a.

1157 Zimmermann, M., Meir, P., Bird, M. I., Malhi, Y., and Ccahuana, A. J. Q.: Climate dependence
1158 of heterotrophic soil respiration from a soil-translocation experiment along a 3000 m

1159 tropical forest altitudinal gradient, *European Journal of Soil Science*, 60, 895-906,
1160 10.1111/j.1365-2389.2009.01175.x, 2009b.
1161 Zimmermann, M., Leifeld, J., Conen, F., Bird, M. I., and Meir, P.: Can composition and
1162 physical protection of soil organic matter explain soil respiration temperature sensitivity?,
1163 *Biogeochemistry*, 107, 423-436, 10.1007/s10533-010-9562-y, 2012.
1164
1165

1166 **12. Tables and Figures**

1167 **Table 1. Site characteristics.**

Elevation Band m a.s.l.	Habitat	Latitude	Longitude	Mean Annual Temperature °C	Mean Annual Precipitation mm	Bulk density 0-10 cm g cm ⁻³	pH	Soil C:N 0-10 cm	Soil C 0-10 cm %	Mineral Soil Particle Size						Landforms	Plots n	Flux Chambers n
										0-10 cm		10-30 cm		0-10 cm				
										Clay	Silt	Sand	Clay	Silt	Sand			
600-1200	Premontane forest	12°53'43"	71°23'04"	20.5	5318	0.38 ± 0.03 (n = 21)	3.4 ± 0.1	11.3 ± 0.2	7.9 ± 0.5	5.4 ± 0.3	68.8 ± 3.9	25.4 ± 15.9	8.9 ± 1.8	81.0 ± 1.7	10.3 ± 2.5	ridge, slope, flat	3	15
1200-2200	Lower montane forest	13°2'56"	71°37'13"	17.2	2631	0.19 ± 0.03 (n = 17)	3.4 ± 0.1	14.5 ± 0.2	25.2 ± 1.3	3.6 ± 0.4	67.3 ± 4.2	29.3 ± 4.5	7.2 ± 0.4	83.8 ± 0.8	9.0 ± 0.9	ridge, slope, flat	3	15
2200-3200	Upper montane forest	13°11'24"	71°35'13"	10.7	1706	0.41 ± 0.02 (n = 12)	3.9 ± 0.1	16.8 ± 0.4	16.3 ± 1.0	5.1 ± 0.9	57.1 ± 7.9	37.9 ± 8.7	4.4 ± 2.0	46.5 ± 16.2	49.1 ± 18.1	ridge, slope	3	15
3200-3700	Montane grassland	13°07'19"	71°36'54"	9.3	2200	0.36 ± 0.03 (n = 27)	4.1 ± 0.1	12.9 ± 0.4	16.0 ± 1.0	2.6 ± 0.2	54.4 ± 3.0	43.0 ± 3.2	n/a	n/a	n/a	ridge, slope, flat, basin	4	20

1168

1169 **Table 2.** Description of the water-filled pore space and NO₃⁻ addition treatments for the
 1170 laboratory manipulation experiments.

Habitat	Experimental Treatment	Soil Depth	Soil Type	WFPS %	Inorganic N added		Replicate <i>n</i>	
					ng N (g soil) ⁻¹	¹⁵ N Tracer		
WATER-FILLED PORE SPACE								
Premontane forest	90 % WFPS	0-10	mineral	90	200	¹⁵ NH ₄ ⁺ ¹⁵ NO ₃ ⁻	5	
	90 % WFPS	0-10	mineral	90	200	¹⁴ NH ₄ ⁺ ¹⁵ NO ₃ ⁻	5	
	70 % WFPS	0-10	mineral	70	200	¹⁵ NH ₄ ⁺ ¹⁵ NO ₃ ⁻	5	
	70 % WFPS	0-10	mineral	70	200	¹⁴ NH ₄ ⁺ ¹⁵ NO ₃ ⁻	5	
	50 % WFPS	0-10	mineral	50	200	¹⁵ NH ₄ ⁺ ¹⁵ NO ₃ ⁻	5	
	50 % WFPS	0-10	mineral	50	200	¹⁴ NH ₄ ⁺ ¹⁵ NO ₃ ⁻	5	
Lower montane forest	30 % WFPS	0-10	mineral	30	200	¹⁵ NH ₄ ⁺ ¹⁵ NO ₃ ⁻	5	
	30 % WFPS	0-10	mineral	30	200	¹⁴ NH ₄ ⁺ ¹⁵ NO ₃ ⁻	5	
	90 % WFPS	0-10	mineral	90	200	¹⁵ NH ₄ ⁺ ¹⁵ NO ₃ ⁻	5	
	90 % WFPS	0-10	mineral	90	200	¹⁴ NH ₄ ⁺ ¹⁵ NO ₃ ⁻	5	
	70 % WFPS	0-10	mineral	70	200	¹⁵ NH ₄ ⁺ ¹⁵ NO ₃ ⁻	5	
	70 % WFPS	0-10	mineral	70	200	¹⁴ NH ₄ ⁺ ¹⁵ NO ₃ ⁻	5	
Upper montane forest	50 % WFPS	0-10	mineral	50	200	¹⁵ NH ₄ ⁺ ¹⁵ NO ₃ ⁻	5	
	50 % WFPS	0-10	mineral	50	200	¹⁴ NH ₄ ⁺ ¹⁵ NO ₃ ⁻	5	
	30 % WFPS	0-10	mineral	30	200	¹⁵ NH ₄ ⁺ ¹⁵ NO ₃ ⁻	5	
	30 % WFPS	0-10	mineral	30	200	¹⁴ NH ₄ ⁺ ¹⁵ NO ₃ ⁻	5	
	90 % WFPS	10-20	mineral	90	20	¹⁵ NH ₄ ⁺ ¹⁵ NO ₃ ⁻	5	
	90 % WFPS	10-20	mineral	90	20	¹⁴ NH ₄ ⁺ ¹⁵ NO ₃ ⁻	5	
Montane grassland	70 % WFPS	10-20	mineral	70	20	¹⁵ NH ₄ ⁺ ¹⁵ NO ₃ ⁻	5	
	70 % WFPS	10-20	mineral	70	20	¹⁴ NH ₄ ⁺ ¹⁵ NO ₃ ⁻	5	
	50 % WFPS	10-20	mineral	50	20	¹⁵ NH ₄ ⁺ ¹⁵ NO ₃ ⁻	5	
	50 % WFPS	10-20	mineral	50	20	¹⁴ NH ₄ ⁺ ¹⁵ NO ₃ ⁻	5	
	30 % WFPS	10-20	mineral	30	20	¹⁵ NH ₄ ⁺ ¹⁵ NO ₃ ⁻	5	
	30 % WFPS	10-20	mineral	30	20	¹⁴ NH ₄ ⁺ ¹⁵ NO ₃ ⁻	5	
NITRATE ADDITION	Premontane forest	control	0-10	mineral	80	n/a	n/a	5
		+50 % background NO ₃ ⁻	0-10	mineral	80	780 ± 60	K ¹⁵ NO ₃	5
		+100 % background NO ₃ ⁻	0-10	mineral	80	1570 ± 120	K ¹⁵ NO ₃	5
	Lower montane forest	+150 % background NO ₃ ⁻	0-10	mineral	80	2350 ± 170	K ¹⁵ NO ₃	5
		control	0-10	mineral	80	n/a	n/a	5
		+50 % background NO ₃ ⁻	0-10	mineral	80	700 ± 60	K ¹⁵ NO ₃	5
	Upper montane forest	+100 % background NO ₃ ⁻	0-10	mineral	80	1400 ± 120	K ¹⁵ NO ₃	5
		+150 % background NO ₃ ⁻	0-10	mineral	80	2100 ± 180	K ¹⁵ NO ₃	5
		control	0-10	organic	80	n/a	n/a	5
	Montane grassland	+50 % background NO ₃ ⁻	0-10	organic	80	90 ± 20	K ¹⁵ NO ₃	5
		+100 % background NO ₃ ⁻	0-10	organic	80	180 ± 50	K ¹⁵ NO ₃	5
		+150 % background NO ₃ ⁻	0-10	organic	80	270 ± 70	K ¹⁵ NO ₃	5
		control	10-20	mineral	80	n/a	n/a	5
		+50 % background NO ₃ ⁻	10-20	mineral	80	90 ± 40	K ¹⁵ NO ₃	5
		+100 % background NO ₃ ⁻	10-20	mineral	80	190 ± 70	K ¹⁵ NO ₃	5
Montane grassland	+150 % background NO ₃ ⁻	10-20	mineral	80	280 ± 110	K ¹⁵ NO ₃	5	
	control	0-10	mineral	80	n/a	n/a	5	
	+50 % background NO ₃ ⁻	0-10	mineral	80	30 ± 10	K ¹⁵ NO ₃	5	
	+100 % background NO ₃ ⁻	0-10	mineral	80	60 ± 20	K ¹⁵ NO ₃	5	
	+150 % background NO ₃ ⁻	0-10	mineral	80	90 ± 40	K ¹⁵ NO ₃	5	

1171

1172 **Table 3.** Seasonal patterns in net N₂O flux, net inorganic N flux, and environmental variables.
 1173 Lower case letters indicate difference among seasons within habitats (*t*-Test on Box-Cox
 1174 transformed data, *P* < 0.05). Values reported here are means and standard errors.

Habitat	N ₂ O mg N-N ₂ O m ⁻² d ⁻¹		WFPS %		Soil Temperature °C		Air Temperature °C		Oxygen %		NO ₃ ⁻ μg N-NO ₃ ⁻ (g resin) ⁻¹ d ⁻¹		NH ₄ ⁺ μg N-NH ₄ ⁺ (g resin) ⁻¹ d ⁻¹	
	Wet Season	Dry Season	Wet Season	Dry Season	Wet Season	Dry Season	Wet Season	Dry Season	Wet Season	Dry Season	Wet Season	Dry Season	Wet Season	Dry Season
Premontane	0.71 ± 0.25 a n = 130	0.79 ± 0.26 a n = 98	51.9 ± 1.6 a n = 135	51.2 ± 2.1 a n = 135	20.7 ± 0.1 a n = 143	20.2 ± 0.1 b n = 120	21.5 ± 0.3 n = 143	20.4 ± 0.5 n = 120	19.4 ± 0.2 a n = 52	19.6 ± 0.2 a n = 36	23.2 ± 3.6 a n = 89	22.1 ± 2.1 a n = 96	31.4 ± 13.0 n = 90	11.3 ± 1.8 n = 95
Lower montane	0.09 ± 0.08 a n = 212	1.02 ± 0.58 b n = 137	42.2 ± 1.0 a n = 271	34.0 ± 1.4 b n = 179	18.1 ± 0.1 a n = 254	17.3 ± 0.2 b n = 164	18.9 ± 0.3 n = 254	18.3 ± 0.2 n = 164	19.2 ± 0.2 a n = 146	19.2 ± 0.1 a n = 81	11.8 ± 1.9 a n = 123	7.8 ± 1.4 a n = 94	20.2 ± 5.4 n = 124	8.6 ± 0.9 n = 93
Upper montane	0.06 ± 0.09 a n = 207	0.01 ± 0.11 a n = 146	42.0 ± 1.3 a n = 264	24.3 ± 1.4 b n = 180	11.8 ± 0.1 a n = 255	10.9 ± 0.2 b n = 165	12.8 ± 0.2 n = 255	12.5 ± 0.3 n = 165	18.7 ± 0.2 a n = 165	18.5 ± 0.2 a n = 109	1.4 ± 0.2 a n = 128	0.6 ± 0.2 b n = 91	22.5 ± 6.3 n = 129	11.3 ± 1.4 n = 93
Montane grassland	-0.01 ± 0.11 a n = 238	0.19 ± 0.12 a n = 160	88.5 ± 0.3 a n = 303	88.3 ± 0.5 a n = 184	11.6 ± 0.1 a n = 282	9.0 ± 0.2 b n = 205	11.4 ± 0.3 n = 284	12.0 ± 0.5 n = 205	12.2 ± 0.9 a n = 176	15.4 ± 0.8 b n = 117	1.5 ± 0.4 a n = 128	2.1 ± 0.4 a n = 81	17.8 ± 4.3 n = 135	7.2 ± 0.8 n = 84

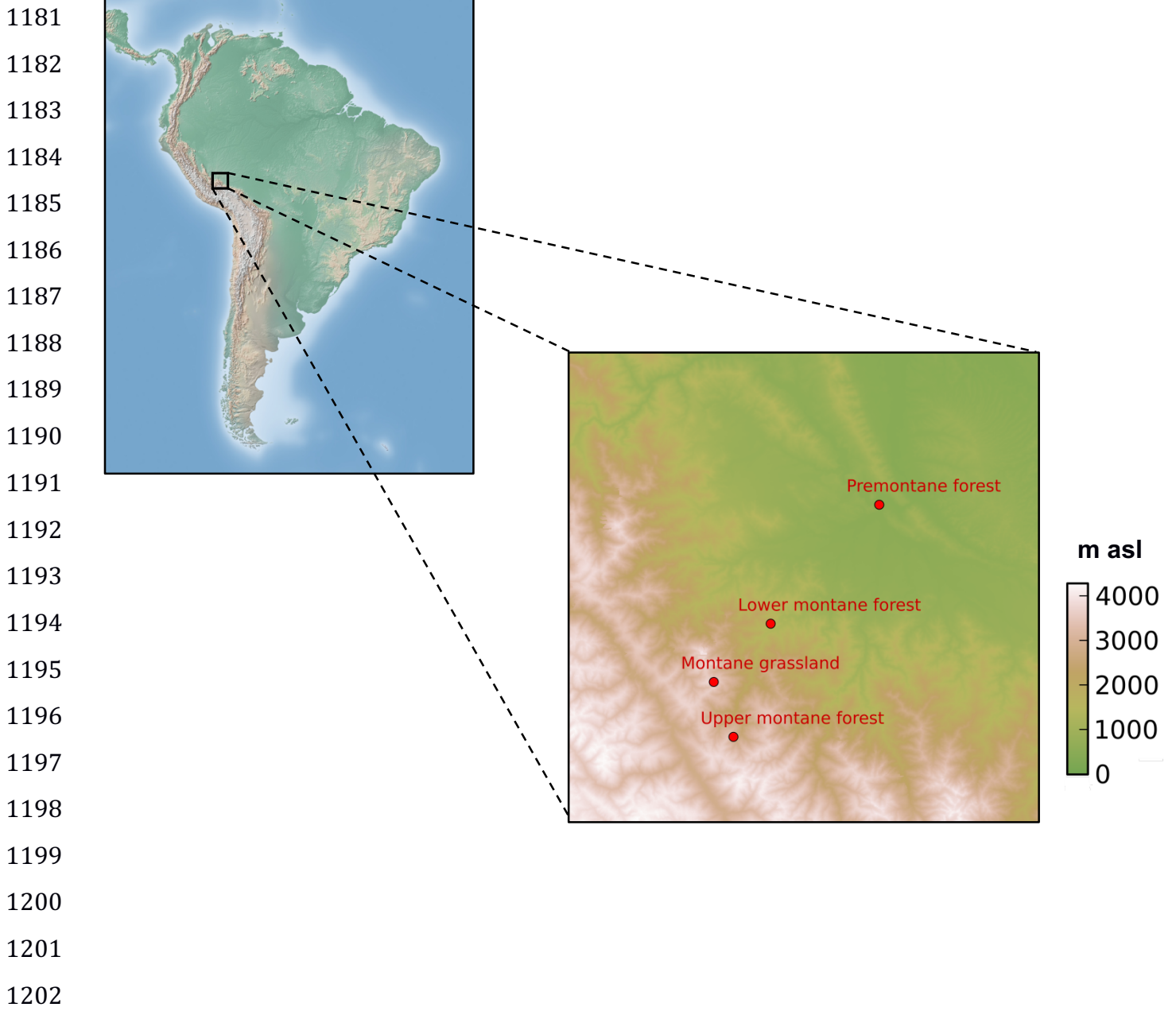
1175
1176

1177 **Table 4.** Area- and seasonally-weighted annual estimates of N₂O, N₂, and total gaseous N
 1178 flux

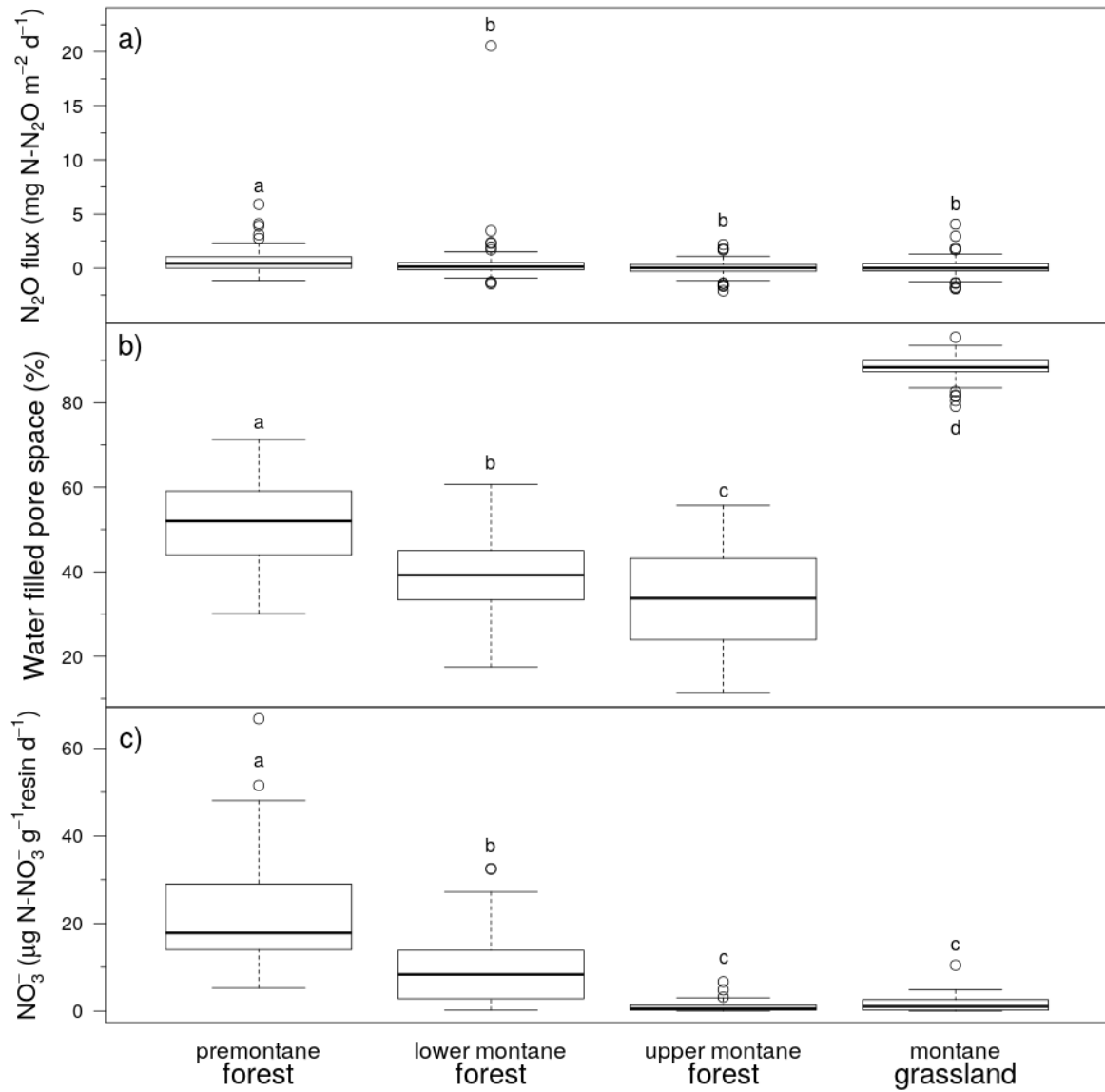
Elevation Band (m.a.s.l.)	Habitat	Surface Area (ha)	Fraction of Land Area		Fraction of Year		Nitrous Oxide Yield		Unweighted Nitrous Oxide Flux		Area-weighted Nitrous Oxide Flux		Area-weighted and Seasonally-weighted Annual Estimate of N ₂ O Flux		Area-weighted and Seasonally-weighted Annual Estimate of N ₂ Flux		Area-weighted and Seasonally-weighted Annual Estimate of Total Gaseous N Flux		
			Wet Season	Dry Season	Wet Season	Dry Season	Wet Season	Dry Season	Wet Season	Dry Season	Wet Season	Dry Season	Wet Season	Dry Season	Wet Season	Dry Season	Wet Season	Dry Season	Wet Season
600-1200	Premontane forest	733000	0.24	0.58	0.42	0.42	0.4 ± 0.05	2.88 ± 0.95	0.63 ± 0.22	0.70 ± 0.23	0.66 ± 0.16	1.00 ± 0.29	1.00 ± 0.29	1.00 ± 0.29	1.00 ± 0.29	1.00 ± 0.29	1.00 ± 0.29	1.00 ± 0.29	1.00 ± 0.29
1200-2200	Lower montane forest	892000	0.30	0.58	0.42	0.42	0.19 ± 0.04	3.72 ± 2.12	0.10 ± 0.09	1.10 ± 0.63	0.52 ± 0.27	2.21 ± 1.24	2.21 ± 1.24	2.21 ± 1.24	2.21 ± 1.24	2.21 ± 1.24	2.21 ± 1.24	2.21 ± 1.24	2.21 ± 1.24
2200-3200	Upper montane forest	807000	0.27	0.58	0.42	0.42	0.42 ± 0.05	0.04 ± 0.40	0.06 ± 0.09	0.01 ± 0.11	0.04 ± 0.07	0.05 ± 0.09	0.05 ± 0.09	0.05 ± 0.09	0.05 ± 0.09	0.05 ± 0.09	0.05 ± 0.09	0.05 ± 0.09	0.05 ± 0.09
3200-3700	Montane grasslands	586000	0.19	0.58	0.42	0.42	0.61 ± 0.06	0.69 ± 0.44	-0.01 ± 0.08	0.13 ± 0.09	0.05 ± 0.06	0.03 ± 0.04	0.03 ± 0.04	0.03 ± 0.04	0.03 ± 0.04	0.03 ± 0.04	0.03 ± 0.04	0.03 ± 0.04	0.03 ± 0.04
Totals		3020000									1.27 ± 0.33	3.29 ± 1.27	3.29 ± 1.27	3.29 ± 1.27	3.29 ± 1.27	3.29 ± 1.27	3.29 ± 1.27	3.29 ± 1.27	4.57 ± 1.31

1179

1180 **Figure 1.** Map of study sites across the Kosñipata Valley, Manu National Park, Peru.



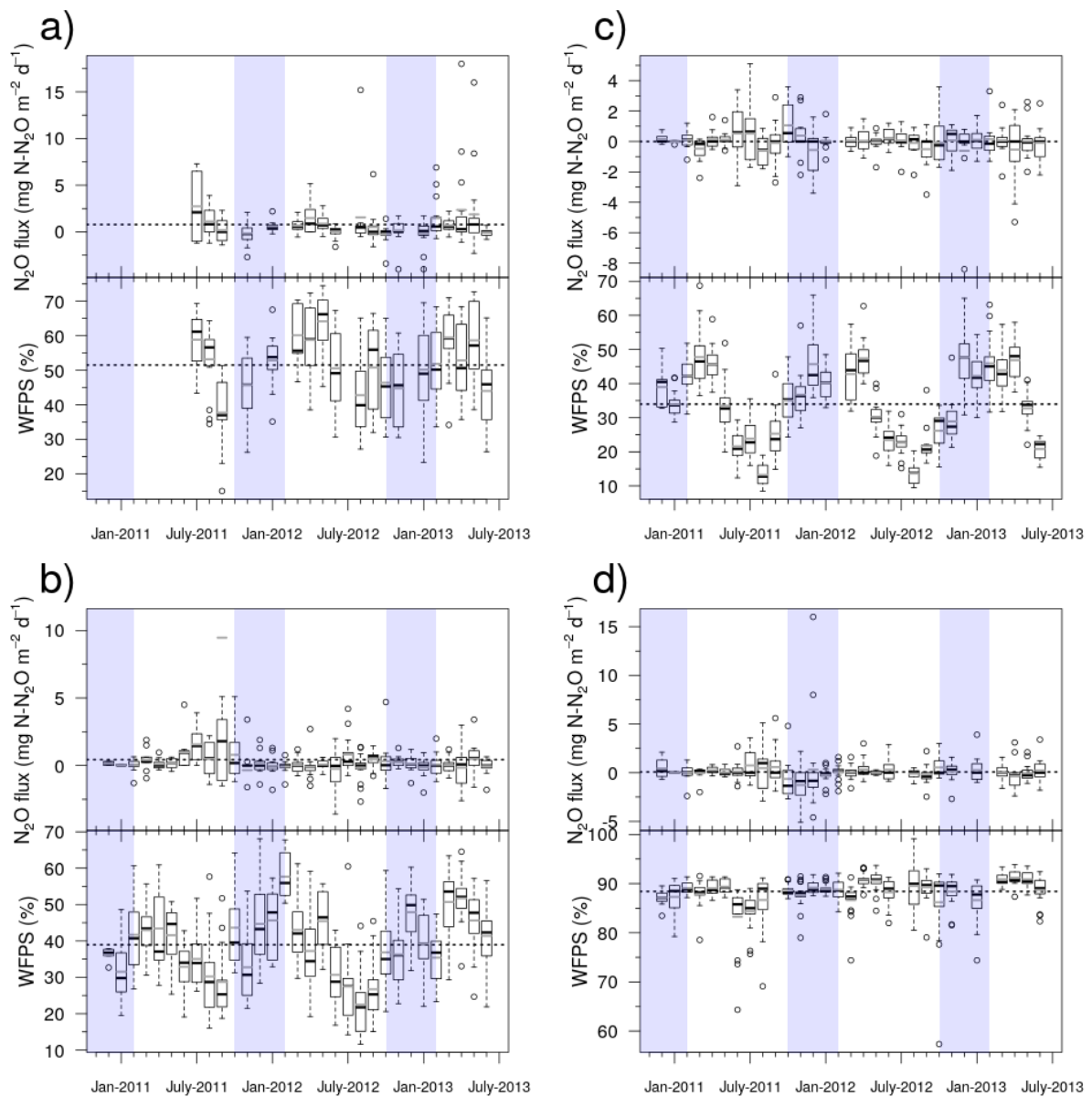
1203 **Figure 2.** Plot-averaged (a) net N₂O flux, (b) water-filled pore space, and (c) resin-extractable
 1204 NO₃⁻ flux among habitats. Boxes enclose the interquartile range, whiskers indicate the 90th
 1205 and 10th percentiles. Lower case letters indicate statistically significant differences among
 1206 means (Fisher's LSD, *P* < 0.05).



1207

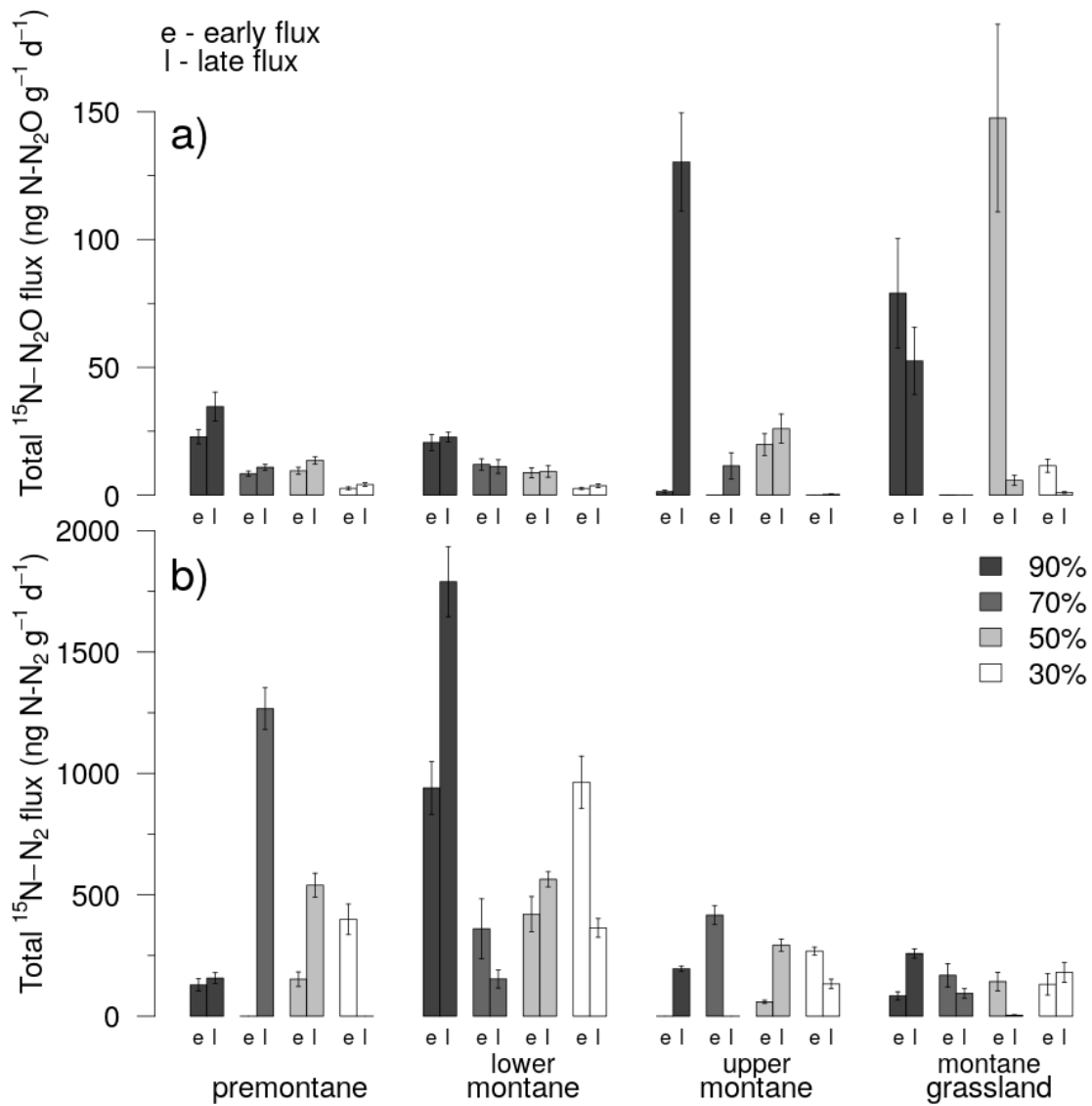
1208

1209 **Figure 3.** Time series of net N₂O flux and water-filled pore space (WFPS). Panels indicate data
 1210 for (a) premontane forest, (b) lower montane forest, (c) upper montane forest, and (d)
 1211 montane grasslands for the 30-month study period beginning in January 2011 and ending in
 1212 June 2013. The broken horizontal line running across each panel denotes the overall mean
 1213 N₂O flux or WFPS for that habitat. The dashed line in each box indicate median values and
 1214 the black lines indicate means. Dry and wet seasons are denoted by vertical shading on the
 1215 graph, with the dry season (May to September) highlighted in white and the wet season
 1216 (October to April) in light blue.



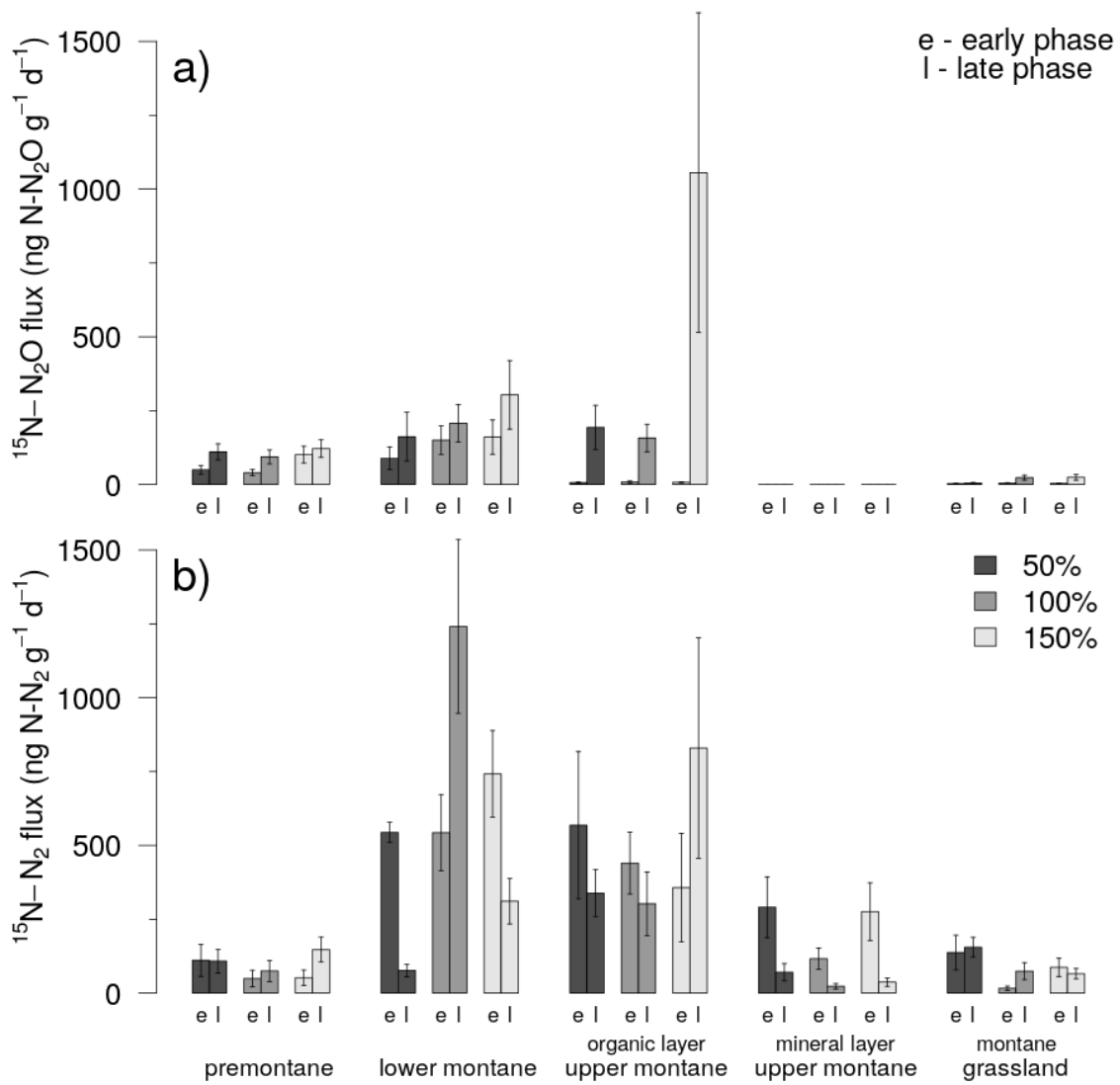
1217
 1218

1219 **Figure 4.** Total (a) $^{15}\text{N-N}_2\text{O}$ flux and (b) $^{15}\text{N-N}_2$ flux during the early (≤ 24 hours) and late (> 24
 1220 hours) incubation phases of the water-filled pore space (WFPS) experiment. Results from the
 1221 90 % WFPS treatment are shown in dark-grey, while data from the 70 %, 50 %, and 30 %
 1222 WFPS treatments are shown in mid-grey, light-grey, and white, respectively. The bar charts
 1223 show means and standard errors.



1224
 1225

1226 **Figure 5.** (a) $^{15}\text{N-N}_2\text{O}$ flux and (b) $^{15}\text{N-N}_2$ flux during the early (≤ 24 hours) and late (> 24 hours) incubation phases of the NO_3^- addition experiment. Results from the +50 % NO_3^- addition are shown in dark-grey, while data from the +100 % and +150 % treatments are shown in mid-grey and light-grey, respectively. The bar charts show means and standard errors.



1230